Journal of Molecular Structure 1248 (2022) 131476

Contents lists available at ScienceDirect

Journal of Molecular Structure

journal homepage: www.elsevier.com/locate/molstr

Potential bacterial biofilm, MRSA, and DHFR inhibitors based on new morpholine-linked chromene-thiazole hybrids: One-pot synthesis and in silico study

Sherif M.H. Sanad[a,*], Ahmed E.M. Mekky[a], Tamer T. El-Idreesy[a,b]

[a] Chemistry Department, Faculty of Science, Cairo University, Giza 12613, Egypt
[b] Department of Chemistry, School of Sciences and Engineering, The American University in Cairo, New Cairo 11835, Egypt

ARTICLE INFO

Article history:
Received 23 July 2021
Revised 3 September 2021
Accepted 8 September 2021
Available online 10 September 2021

Keywords:
Bacterial biofilm inhibitors
DHFR inhibitors
Morpholine-thiazole hybrids
MRSA inhibitors
SwissADME prediction

ABSTRACT

We report herein the utility of the morpholine-linked benzaldehyde as a key building block in the preparation of two series of new chromene-thiazoles with potential bioactivities. In this regard, a one-pot protocol was developed involving the reaction of the prior aldehyde, 2-cyanothioacetamide and α-bromoketones in dioxane in the presence of triethylamine to give the target hybrids. Thiazole hybrids **9d** and **9e**, attached to two chromene units at thiazole-C2 and C4, and linked to methyl or methoxy groups, respectively, showed the best antibacterial activity. The previous hybrids exhibited MIC/MBC values of 3.9/7.8 and 1.7/3.5 µM, respectively, against *S. aureus, S. mutans* and *E. coli* strains. In addition, the same hybrids gave MIC values of 7.7–32.0 µM and MBC values of 15.5–64.1, µM against MRSA ATCC:33,591 and ATCC:43,300 strains. Furthermore, **9d** and **9e** gave the best bacterial biofilm inhibitory activity against *S. aureus, S. mutans* and *E. coli* strains with IC_{50} values ranging from 3.9 to 4.6 µM. Also, **9e** and **9d** displayed superior dihydrofolate reductase enzyme inhibitory activity with IC_{50} values of 0.122 and 0.131 µM, respectively, compared to the standard sulfadiazine (IC_{50} value of 0.138 µM). Molecular docking study was used to determine the binding energies of some new hybrids with the previous enzyme. Moreover, physicochemical, pharmacokinetic properties, and drug-likeness of some new hybrids were calculated using SwissADME.

1. Introduction

The ability of the dihydrofolate reductase (DHFR) enzyme as a therapeutic target in the treatment of infections has been demonstrated since the middle of the last century [1]. Using NADPH, DHFR catalyzes the reduction of dihydrofolate to tetrahydrofolate and is involved in the synthesis of cell proliferation raw material, both in prokaryotic and eukaryotic cells [2]. DHFR inhibitors are widely used in the treatment of fungal, bacterial and mycobacterial infections and in the fight against malaria and other protozoal infections as well as fight against cancer [3–6]. These include pyrimethamine and proguanil as antimalarial drugs [7]; trimethoprim, a widely used sulfonamide-associated antibacterial medication such as sulfamethoxazole [8,9]; and methotrexate, the first discovered anticancer agent that act by inhibition of DHFR [10].

Morpholine is commonly used in industry as well as in the synthesis of various biologically active organic derivatives [11,12]. Various morpholine derivatives can be isolated from naturally occurring sources [13] These include Polygonapholine extracted from the rhizome methanol extract of *Polygonatum altelobatum* and used as a tonic drink in Taiwan [14], as well as Lidamycin isolated from *Streptomyces globisporus* and used as an antitumor antibiotic [15]. Numerous publications reported the synthesis of heterocyclic derivatives incorporating morpholine units [16,17]. This is attributed to the wide spectrum of medicinal applications of these derivatives including antidepressant [18,19], appetite suppressant [20], antitumor [21], antioxidant activities [22,23]. They also act selective inhibitors of acetylcholinesterase [24,25], monoamine oxidase A and B [25], cyclooxygenase-1 and 2 [25], and glucosidase enzymes [26]. In addition, morpholine units are frequently selected as key synthons for different biologically important derivatives including the preparation of enantiomerically pure α-amino acids, β-amino alcohols, and peptides [27–29].

Thiazole derivatives have shown remarkable antimicrobial [30], anti-inflammatory, analgesic [31], anticancer [32], antihypertensive [33], anti-HIV [34], anti-hypoxic [35], and anti-asthmatic activities [36]. Moreover, chromene hybrids act as antimicrobial [37], anti-inflammatory, analgesic [38], antioxidant [39], and antifungal [40],

* Corresponding author.
E-mail address: sherif_hamed1980@yahoo.com (S.M.H. Sanad).

https://doi.org/10.1016/j.molstruc.2021.131476
0022-2860/

anti-hepatitis C virus [41], antitumor activities [42], and promising acetylcholinesterase inhibitors [43,44]. Fig. 1 represents some important morpholine-based drugs [45–47], in addition to some promising DHFR inhibitors incorporating a thiazole or chromene unit [48–50]. Based on the aforementioned findings and in connection with our efforts to prepare potential antibacterial agents as well as DHFR inhibitors [51–59], we designed herein facile synthetic routes for the preparation of novel thiazole-chromene hybrids incorporating a morpholine unit.

A pharmacophore can be defined by determining complementarities between a ligand and its corresponding binding site [60]. A pharmacophore's most important elements can range from a group of atoms to a portion of the molecule's volume. Hydrophobic and/or aromatic rings, as well as hydrogen bond acceptors and/or donors, are key features of a pharmacophore [61]. Sulfadiazine, a reference DHFR inhibitor, contains a sulfonamide group and a pyrimidine-N atom, both of which act as hydrogen bond acceptors to the DHFR binding sites [60]. Our designed new hybrids have the same pharmacophoric elements as sulfadiazine due to the chromene-CO group(s) and morpholine-O atom. Fig. 2 compares the pharmacophoric elements of the reference sulfadiazine with **9d** as an example of the designed hybrids.

In this study, the pharmacological activities of the new morpholine-linked thiazole-chromene hybrids as potential bacterial biofilm, MRSA and DHFR inhibitors were tested. Furthermore, the SwissADME program was used to calculate the physicochemical, pharmacokinetic, and medicinal chemistry properties of some new hybrids, as well as their drug-likeness.

2. Experimental

2.1. Materials

All solvents were acquired from commercial sources and used as received unless otherwise stated. All other chemicals were acquired from Merck or Aldrich and used without further purification. The melting points were measured on a Stuart melting point apparatus and are uncorrected. IR spectra were recorded on a Smart iTR, which is an ultra-high-performance, versatile Attenuated Total Reflectance (ATR) sampling accessory on the Nicolet iS10 FT-IR spectrometer. NMR spectra were recorded on Bruker Avance III 400 MHz spectrophotometer (400 MHz for ^{1}H and 100 MHz for ^{13}C) using TMS as an internal standard and DMSO–d_6 as solvent and chemical shifts were expressed as δ ppm units. Mass spectra were recorded on a GC–MS-QP1000EX spectrometer using inlet type at 70 eV. Elemental analyses were carried out on a EuroVector instrument C, H, N, S analyzer EA3000 Series. All spectral analyses as well as the biological screening were conducted in the laboratories of Cairo University.

2.2. The procedures and spectral data

2.2.1. Synthesis of 2-imino-6-(morpholinomethyl)–2H-chromene-3-carbothioamide (5)

A mixture of 2-hydroxybenzaldehyde **3** (5 mmol) and 2-cyanothioacetamide **4** (5 mmol) in ethanol (15 mL) in the presence of four drops of piperidine was boiled at reflux for 3 h to give a sole product as detected by TLC analysis. The reaction was cooled, filtrated, washed with cold ethanol and the reaction product was recrystallized from dioxane / ethanol mixture as pale yellow powders (78%); m.p. 188 °C; IR (υ cm^{-1}): 3404, 3316, 3170 (NH, NH$_2$); ^{1}H NMR (DMSO–d_6): δ 2.44 (t, J = 4.8 Hz, 4H, morpholine-NCH$_2$), 3.61 (t, J = 4.8 Hz, 4H, morpholine–OCH$_2$), 3.66 (s, 2H, CH$_2$), 7.18 (d, J = 8.4 Hz, 1H, H8), 7.30 (d, J = 8.4 Hz, 1H, H7), 7.63 (s, 1H, H5), 8.24 (s, 1H, H4), 8.78, 9.00 (s, 2H, NH$_2$), 10.13 (s, 1H, NH); ^{13}C NMR (DMSO–d_6): δ 53.8, 60.9, 66.5, 117.0, 121.1, 122.1, 127.6, 131.3, 137.2, 145.8, 150.9, 157.1, 196.2; MS m/z (%): 303 (M^+, 59.2); Anal. for $C_{15}H_{17}N_3O_2S$: C, 59.39; H, 5.65; N, 13.85; found: C, 59.21; H, 5.47; N, 13.94%.

2.2.2. Synthesis of thiazole-chromene hybrids 7 and 9

2.2.2.1. Method 'A' (synthesis of hybrid 7a). A mixture of 2-imino-2*H*-chromene-3-carbothioamide **5** (5 mmol) and 2–bromo-1-phenylethan-1-one **6a** (5 mmol) in dioxane (15 mL) in the presence of four drops of piperidine was boiled at reflux for 3 h to afford a sole product as detected by TLC analysis. The reaction was cooled, filtrated, washed with cold ethanol and the reaction product was recrystallized from dioxane / ethanol mixture.

2.2.2.2. Method 'B' (one-pot protocol). A ternary mixture of 2-hydroxybenzaldehyde **3** (5 mmol), 2-cyanothioacetamide **4** (5 mmol) and the appropriate of α-bromoketones **6a 6e** or **8a 8e** (5 mmol) in dioxane (15 mL) in the presence of triethylamine (0.4 mL) was boiled at reflux for 6–8 h to give a sole product in each case as detected by TLC analyses. The reaction was cooled, filtrated, washed with cold ethanol and the reaction product was recrystallized from the proper solvent.

2.2.3. 6-(Morpholinomethyl)–3-(4-phenylthiazol-2-yl)–2H-chromen-2-one (7a)

Pale yellow powders (dioxane / ethanol mixture, 70% using method 'A'; 85% using method 'B'); m.p. 210 °C; IR (υ cm^{-1}): 1716 (CO); ^{1}H NMR (DMSO–d_6): δ 2.40 (t, J = 4.8 Hz, 4H, morpholine-NCH$_2$), 3.60 (t, J = 4.8 Hz, 4H, morpholine–OCH$_2$), 3.65 (s, 2H, CH$_2$), 7.22–7.25 (m, 2H, H7 and H8), 7.32–7.38 (m, 3H, Ar-H's), 7.66 (s, 1H, H5), 7.85 (d, J = 8.4 Hz, 2H, Ar-H's), 7.93 (s, 1H, thiazole-H), 8.34 (s, 1H, H4); ^{13}C NMR (DMSO–d_6): δ 53.5, 60.6, 66.3, 113.2, 117.2, 118.1, 122.4, 124.2, 126.8, 128.5, 129.0, 131.5, 132.0, 132.4, 144.3, 147.2, 151.3, 160.4, 164.6; MS m/z (%): 404 (M^+, 47.3); Anal. for $C_{23}H_{20}N_2O_3S$: C, 68.30; H, 4.98; N, 6.93; found: C, 68.42; H, 5.11; N, 7.05%.

2.2.4. 3-(4-(4-Chlorophenyl)thiazol-2-yl)–6-(morpholinomethyl)–2H-chromen-2-one (7b)

Pale yellow powders (dioxane, 77%); m.p. 234–236 °C; IR (υ cm^{-1}): 1717 (CO); ^{1}H NMR (DMSO–d_6): δ 2.43 (t, J = 4.8 Hz, 4H, morpholine-NCH$_2$), 3.58 (t, J = 4.8 Hz, 4H, morpholine–OCH$_2$), 3.63 (s, 2H, CH$_2$), 7.24–7.27 (m, 2H, H7 and H8), 7.45 (d, J = 8.4 Hz, 2H, Ar-H's), 7.62 (s, 1H, H5), 7.89 (d, J = 8.4 Hz, 2H, Ar-H's), 7.96 (s, 1H, thiazole-H), 8.38 (s, 1H, H4); ^{13}C NMR (DMSO–d_6): δ 53.6, 60.8, 66.4, 113.4, 117.0, 118.2, 122.6, 124.4, 127.5, 128.7, 131.4, 132.3, 132.7, 135.6, 144.2, 146.6, 150.8, 159.8, 164.8; Anal. for $C_{23}H_{19}ClN_2O_3S$ (438.9): C, 62.94; H, 4.36; N, 6.38; found: C, 63.10; H, 4.45; N, 6.27%.

2.2.5. 3-(4-(4-Bromophenyl)thiazol-2-yl)–6-(morpholinomethyl)–2H-chromen-2-one (7c)

Pale yellow powders (dioxane, 79%); m.p. 246 °C; IR (υ cm^{-1}): 1718 (CO); ^{1}H NMR (DMSO–d_6): δ 2.40 (t, J = 4.8 Hz, 4H, morpholine-NCH$_2$), 3.57 (t, J = 4.8 Hz, 4H, morpholine–OCH$_2$), 3.63 (s, 2H, CH$_2$), 7.20 (d, J = 8.4 Hz, 1H, H7), 7.28 (d, J = 8.4 Hz, 1H, H8), 7.49 (d, J = 8.4 Hz, 2H, Ar-H's), 7.64 (s, 1H, H5), 7.80 (d, J = 8.4 Hz, 2H, Ar-H's), 8.00 (s, 1H, thiazole-H), 8.33 (s, 1H, H4); ^{13}C NMR (DMSO–d_6): δ 53.5, 60.6, 66.5, 113.3, 117.2, 117.9, 121.9, 122.8, 124.7, 126.5, 131.3, 131.6, 131.8, 132.0, 144.3, 145.6, 150.4, 159.3, 164.7; Anal. for $C_{23}H_{19}BrN_2O_3S$ (483.3): C, 57.15; H, 3.96; N, 5.80; found: C, 57.02; H, 4.13; N, 5.96%.

2.2.6. 6-(Morpholinomethyl)–3-(4-(p-tolyl)thiazol-2-yl)–2H-chromen-2-one (7d)

Pale yellow powders (dioxane / ethanol mixture, 84%); m.p. 208–210 °C; IR (υ cm^{-1}): 1716 (CO); ^{1}H NMR (DMSO–d_6): δ 2.36

(s, 3H, *p*-CH_3), 2.43 (t, J = 4.8 Hz, 4H, morpholine-NCH_2), 3.59 (t, J = 4.8 Hz, 4H, morpholine–OCH_2), 3.65 (s, 2H, CH_2), 7.18–7.21 (m, 2H, H7 and H8), 7.30 (d, J = 8.4 Hz, 2H, Ar-H's), 7.61 (s, 1H, H5), 7.74 (d, J = 8.4 Hz, 2H, Ar-H's), 7.96 (s, 1H, thiazole-H), 8.41 (s, 1H, H4); ^{13}C NMR (DMSO–d_6): δ 20.5, 53.4, 60.5, 66.6, 113.2, 116.8, 118.2, 121.7, 124.4, 127.2, 128.8, 131.2, 131.4, 131.9, 139.3, 144.8, 146.3, 150.8, 159.8, 164.5; MS *m/z* (%): 418 (M^+, 52.8); Anal. for $C_{24}H_{22}N_2O_3S$: C, 68.88; H, 5.30; N, 6.69; found: C, 69.04; H, 5.45; N, 6.78%.

2.2.7. 3-(4-(4-Methoxyphenyl)thiazol-2-yl)–6-(morpholinomethyl)–2H-chromen-2-one (7e)

Pale yellow powders (dioxane, 80%); m.p. 230 °C; IR (υ cm^{-1}): 1717 (CO); ^{1}H NMR (DMSO–d_6): δ 2.41 (t, J = 4.8 Hz, 4H, morpholine-NCH_2), 3.57 (t, J = 4.8 Hz, 4H, morpholine–OCH_2), 3.61 (s, 2H, CH_2), 3.83 (s, 3H, *p*–OCH_3), 6.95 (d, J = 8.4 Hz, 2H, Ar-H's), 7.20 (d, J = 8.4 Hz, 1H, H7), 7.27 (d, J = 8.4 Hz, 1H, H8), 7.64 (s, 1H, H5), 7.79 (d, J = 8.4 Hz, 2H, Ar-H's), 7.99 (s, 1H, thiazole-H), 8.36 (s, 1H, H4); ^{13}C NMR (DMSO–d_6): δ 53.6, 55.3, 60.7, 66.8, 112.9, 114.1, 116.9, 118.3, 122.0, 124.2, 127.2, 129.5, 131.4, 132.3, 144.5, 146.1, 150.7, 159.7, 160.1, 164.6; Anal. for $C_{24}H_{22}N_2O_4S$ (434.5): C, 66.34; H, 5.10; N, 6.45; found: C, 66.17; H, 4.98; N, 6.37%.

2.2.8. 6-(Morpholinomethyl)–3-(4-(2-oxo-2H-chromen-3-yl)thiazol-2-yl)–2H-chromen-2-one (9a)

Beige powders (dioxane, 77%); m.p. 260–262 °C; IR (υ cm^{-1}): 1728, 1696 (CO); ^{1}H NMR (DMSO–d_6): δ 2.42 (t, J = 4.8 Hz, 4H, morpholine-NCH_2), 3.59 (t, J = 4.8 Hz, 4H, morpholine–OCH_2), 3.63 (s, 2H, CH_2), 7.19–7.22 (m, 2H, H7 and H8), 7.36–7.42 (m, 2H, H6′ and H8′), 7.56–7.60 (m, 2H, H5 and H7′), 7.82 (d, J = 8.8 Hz, 1H, H5′), 7.90 (s, 1H, thiazole-H), 8.35 (s, 1H, H4), 8.48 (s, 1H, H4′); ^{13}C NMR (DMSO–d_6): δ 53.5, 60.6, 66.6, 114.2, 115.3, 116.6, 117.6, 117.8, 118.3, 123.4, 125.7, 128.5, 128.8, 129.6, 130.2, 134.3, 134.6, 144.8, 148.7, 150.2, 151.3, 162.1, 163.2, 165.3; MS *m/z* (%): 472 (M^+, 40.5); Anal. for $C_{26}H_{20}N_2O_5S$: C, 66.09; H, 4.27; N, 5.93; found: C, 65.87; H, 4.34; N, 6.08%.

2.2.9. 6-Chloro-3-(2-(6-(morpholinomethyl)–2-oxo-2H-chromen-3-yl)thiazol-4-yl)–2H-chromen-2-one (9b)

Beige powders (DMF / ethanol mixture, 74%); m.p. 274 °C; IR (υ cm^{-1}): 1729, 1697 (CO); ^{1}H NMR (DMSO–d_6): δ 2.40 (t, J = 4.8 Hz, 4H, morpholine-NCH_2), 3.60 (t, J = 4.8 Hz, 4H, morpholine–OCH_2), 3.66 (s, 2H, CH_2), 7.18 (d, J = 8.4 Hz, 1H, H7), 7.25 (d, J = 8.4 Hz, 1H, H8), 7.36 (d, J = 8.8 Hz, 1H, H8′), 7.62 (s, 1H, H5), 7.74–7.76 (m, 2H, H5′ and H7′), 7.94 (s, 1H, thiazole-H), 8.28 (s, 1H, H4), 8.34 (s, 1H, H4′); ^{13}C NMR (DMSO–d_6): δ 53.3, 60.4, 66.5, 114.2, 117.2, 117.7, 118.0, 118.2, 118.4, 123.2, 128.0, 129.2, 129.4, 130.4, 133.2, 133.9, 134.3, 144.4, 148.9, 151.8, 152.4, 163.0, 163.4, 165.4; Anal. for $C_{26}H_{19}ClN_2O_5S$ (506.9): C, 61.60; H, 3.78; N, 5.53; found: C, 61.73; H, 3.64; N, 5.68%.

2.2.10. 6-Bromo-3-(2-(6-(morpholinomethyl)–2-oxo-2H-chromen-3-yl)thiazol-4-yl)–2H-chromen-2-one (9c)

Beige powders (DMF / ethanol mixture, 78%); m.p. 270–272 °C; IR (υ cm^{-1}): 1724, 1695 (CO); ^{1}H NMR (DMSO–d_6): δ 2.43 (t, J = 4.8 Hz, 4H, morpholine-NCH_2), 3.58 (t, J = 4.8 Hz, 4H, morpholine–OCH_2), 3.63 (s, 2H, CH_2), 7.15 (d, J = 8.8 Hz, 1H, H8′), 7.22 (d, J = 8.4 Hz, 1H, H7), 7.28 (d, J = 8.4 Hz, 1H, H8), 7.60–7.62 (m, 2H, H5 and H7′), 7.90 (s, 1H, thiazole-H), 7.95 (s, 1H, H5′), 8.27 (s, 1H, H4), 8.32 (s, 1H, H4′); ^{13}C NMR (DMSO–d_6): δ 53.4, 60.6, 66.6, 114.3, 117.5, 117.8, 118.0, 118.3, 118.6, 118.8, 123.5, 129.3, 130.2, 130.6, 133.6, 134.4, 135.8, 144.2, 149.2, 151.4, 153.0, 162.8, 163.3, 165.6; Anal. for $C_{26}H_{19}BrN_2O_5S$ (551.4): C, 56.63; H, 3.47; N, 5.08; found: C, 56.49; H, 3.57; N, 4.93%.

2.2.11. 6-Methyl-3-(2-(6-(morpholinomethyl)–2-oxo-2H-chromen-3-yl)thiazol-4-yl)–2H-chromen-2-one (9d)

Beige powders (DMF / ethanol mixture, 72%); m.p. 262–264 °C; IR (υ cm^{-1}): 1730, 1694 (CO); ^{1}H NMR (DMSO–d_6): δ 2.37 (s, 3H, CH_3), 2.42 (t, J = 4.8 Hz, 4H, morpholine-NCH_2), 3.58 (t, J = 4.8 Hz, 4H, morpholine–OCH_2), 3.63 (s, 2H, CH_2), 7.15–7.18 (m, 2H, H7 and H7′), 7.23–7.26 (m, 2H, H8 and H8′), 7.55 (s, 1H, H5′), 7.60 (s, 1H, H5), 7.90 (s, 1H, thiazole-H), 8.24 (s, 1H, H4), 8.40 (s, 1H, H4′); ^{13}C NMR (DMSO–d_6): δ 20.8 (CH_3), 53.5, 60.5, 66.4, 115.0, 116.0, 116.2, 117.2, 117.4, 118.4, 118.7, 126.7, 127.7, 130.2, 133.5, 133.8, 134.3, 134.7, 142.0, 147.7, 151.8, 152.7, 163.5, 164.1, 165.4; Anal. for $C_{27}H_{22}N_2O_5S$ (486.5): C, 66.65; H, 4.56; N, 5.76; found: C, 66.72; H, 4.67; N, 5.53%.

2.2.12. 6-Methoxy-3-(2-(6-(morpholinomethyl)–2-oxo-2H-chromen-3-yl)thiazol-4-yl)–2H-chromen-2-one (9e)

Beige powders (DMF / ethanol mixture, 70%); m.p. 270–272 °C; IR (υ cm^{-1}): 1730, 1698 (CO); ^{1}H NMR (DMSO–d_6): δ 2.42 (t, J = 4.8 Hz, 4H, morpholine-NCH_2), 3.57 (t, J = 4.8 Hz, 4H, morpholine–OCH_2), 3.62 (s, 2H, CH_2), 3.80 (s, 3H, OCH_3), 7.16 (d, J = 8.4 Hz, 1H, H7), 7.21–7.26 (m, 3H, H5′, H7′ and H8), 7.45 (d, J = 8.4 Hz, 1H, H8′), 7.59 (s, 1H, H5), 7.93 (s, 1H, thiazole-H), 8.19 (s, 1H, H4), 8.28 (s, 1H, H4′); ^{13}C NMR (DMSO–d_6): δ 53.4, 55.8, 60.6, 66.2, 113.7, 115.3, 116.4, 116.8, 117.3, 117.5, 117.9, 118.3, 118.6, 127.4, 130.3, 133.0, 133.6, 142.7, 147.3, 149.9, 151.4, 154.7, 163.4, 163.9, 165.2; MS *m/z* (%): 502 (M^+, 36.4); Anal. for $C_{27}H_{22}N_2O_6S$: C, 64.53; H, 4.41; N, 5.57; found: C, 64.38; H, 4.55; N, 5.74%.

2.3. The in vitro antibacterial screening

2.3.1. Minimum inhibitory concentration (MIC) determination

The inhibitory activities were estimated against each of *Staphylococcus aureus* (ATCC:6538), *Streptococcus mutans,* (ATCC:25,175), *Enterococcus faecalis* (ATCC:29,212), *Escherichia coli* (ATCC:9637), *Pseudomonas aeruginosa* (ATCC:27,953) and *Klebsiella pneumonia* (ATCC:10,031)] as well as MRSA (ATCC:33,591 and ATCC:43,300) bacterial strains [62]. MIC values were determined using microbroth serial dilution method [63] in a sterile 96-well microtiter plate after overnight incubation of tested bacteria at 37 °C. This assay was performed in triplicates for consistency in accordance with guidelines provided by CLSI (2012) [64]. Ciprofloxacin (100 µg susceptibility disk) was used as a standard drug. The concentration of the tested hybrids as well as ciprofloxacin used in the study ranged from 250 to 0.9 µg/mL. The sterile Muller-Hinton broth (MHB) was enriched with 2% NaCl before the tested antimicrobial agents were inserted into the well at concentration gradient in a serial dilution. Then the diluted bacterial suspension at final inoculum of 10^6 CFU/mL was added. The tested compound in MHB was used as negative control to ensure medium sterility, while the inoculum in MHB served as positive control to ensure the adequacy of the broth for bacterial growth. To facilitate the observation of the growth of bacteria in each well, 20 µL of 2,3,5-triphenyltetrazolium chloride (TTC) at 2 mg/mL was added into each well.

2.3.2. Minimum bactericidal concentration (MBC)

The tested thiazoles were screened against each of *Staphylococcus aureus* (ATCC:6538), *Streptococcus mutans* (ATCC:25,175) and *E. coli* (ATCC:9637) as well as MRSA (ATCC:33,591 and ATCC:43,300) bacterial strains to estimate their MBC values [65]. Each of the tested strains was cultured in sterile broth medium for 24 h at 37 °C. The assay was performed in 2 mL microcentrifuge tubes with concentrations ranging from 250 to 0.9 µg/mL of the tested derivatives. To each concentration of the tested derivatives, 0.1 mL of the cultured bacterial strain was added and then, allowed to incubate for 24 h at 37 °C. 10 µL sample was collected post incubation and seeded onto the agar plates and left to incubate for 24 h

at 37 °C. All the results were carried out in duplicate and the average values were determined.

2.3.3. Biofilm inhibition assay

The tested thiazoles were screened for their bacterial biofilm inhibitory activities in sterile 96-well polystyrene microtiter plates [66]. The assay was performed against each of *Staphylococcus aureus* (ATCC:6538), *Streptococcus mutans* (ATCC:25,175) and *E. coli* (ATCC:9637) strains. The selected strains were cultured in tryptone soy broth (supplemented with 0.5% glucose) for 24 h. The tested thiazoles (using concentrations in the range from 0 to 250 µg/mL) were mixed with 5×10^5 CFU mL^{-1} concentration of the bacterial suspensions. In each well, 100 µL were distributed and then allowed to incubate at 37 °C for 24 h under static conditions. To remove the non-adherent bacteria, the medium was discarded and then washed with phosphate buffered saline. Each well of the microtiter plate was stained with 100 µL of 0.1% crystal violet solution then allowed to incubate for 30 min at rt. Then, the crystal violet solution was discarded from the plates, washed with distilled water for 3–4 times and left to dry in air at rt. The crystal violet stained biofilm was solubilized in 100 µL of ethanol 95% and the absorbance was measured using spectrophotometer at 540 nm. Blank wells were used as background check. All results were performed in triplicates. The inhibition data were interpreted from the dose-response curves and the IC_{50} values were indicated as mean ± SD.

2.4. Cytotoxicity against eukaryotic cells

2.4.1. Cell line, culture conditions and preparation of compounds

Cytotoxicity was screened against the human breast epithelial MCF-10A, the human breast carcinoma MCF-7, colon cancer Caco2, and liver hepatocellular carcinoma HEPG2 cell lines, which were obtained from Cairo University Research Park (CURP), Faculty of Agriculture. The cell lines were cultivated in Dulbecco's Modified Eagle's Medium (DMEM). All of the growth media were supplemented with 10% Foetal Bovine Serum (FBS) and antibiotics (100 U/mL penicillin and 100 mg/mL streptomycin) at 37 °C in a humidified atmosphere containing 5% CO_2. The tested thiazoles as well as doxorubicin, as a positive control, were dissolved in DMSO and final concentrations were diluted in culture medium.

2.4.2. Neutral red uptake assay (NRU assay)

The NRU assay relies on the ability of living cells to incorporate and bind neutral red, a weak cationic dye, in lysosomes [67]. The tested thiazoles were subjected to evaluation of their cytotoxicity against MCF-10A, MCF-7, Caco2, and HEPG2 cell lines in comparison to the reference doxorubicin. Exponentially growing cells were collected using 0.25% Trypsin-EDTA, then the cell suspension counted using hemocytometer, and cell viability checked by trypan blue (100% viability). Then, an approximately 1.0×10^5 cell/mL of cells suspension was made by dilution with complete medium. 200 µL of this suspension, about ≈20,000 cell/well, was dispensed by multichannel pipette into the inner 60 wells of the 96 well plate and the peripheral wells were filled with PBS. The plate was allowed to incubate for 24 h to allow cells attachment to the plate wall before the addition of the tested hybrids. Different concentrations of the tested thiazoles (5, 25, 50 and 75 µg/mL) were made by using DMEM media. Then, 200 µL of treatment media was dispensed into four replicates for each concentration and other wells were filled with untreated cells only (as a negative control) and wells filled with media containing doxorubicin HCL as a positive control. The 96 well plate allowed to incubate at 37 °C for 48 h. Then, the medium and extracts were discarded and replaced with 100 µL of neutral red solution (50 mg/mL) and centrifuged at 1800 rpm for 10 min to eliminate any crystals of precipitated dye. After three hours of incubation at 37 °C, the dye medium was removed and the microplate was washed twice with 150 µL PBS to eliminate the unabsorbed neutral red dye contained in the wells. Then, the cellular morphology of the treated cell lines with the tested derivatives were detected using Inverted Microscope Leica DMI3000B. Also, the absorbance of acidified ethanol solution containing extracted neutral red dye was calculated *via* microplate reader (BioTek, ELX808) at 540 nm to estimate the optical density and the cell viability% was determined. All results were performed in triplicates. The IC_{50} values were indicated as mean ± SD.

2.5. The in vitro DHFR inhibition assay

The dihydrofolate reductase inhibition assay [68] was performed as per the manual of the DHFR assay kit (Sigma product code CS0340). All the dilutions were made in assay buffer, pH 7.5. Stock solutions of the test compounds with different concentrations were prepared in DMSO, and an amount of 20 µL of each was taken to attain final concentration of 10^{-8}, 10^{-7}, 10^{-6}, 10^{-5} M in the respective wells of 96-well plate containing assay buffer. Methotrexate was diluted to 100-fold dilution with DHFR assay buffer. 2 µL of tested samples (including methotrexate as positive control) was added to wells assigned as the test samples, enzyme control, or inhibitor control. An amount of 0.1 unit of DHFR as supplied in the kit was diluted, and an amount of 2 µL of its 3×10^{-3} unit was added to 798 µL assay buffer, then 98 µL of the diluted DHFR solution was added to each well of the 96-well plate. Wells containing 100 µL of assay buffer were used as background control to check any inhibition of enzyme activity due to solvent. 10 mM stock solution of NADPH in assay buffer was prepared, mixed by vortex and kept on ice, then 40 µL of the diluted NADPH solution was added to wells including the test samples, enzyme control, inhibitor control or background control. Avoiding light, wells were mixed and incubated at room temperature for 10–15 min. 10 mM Stock solutions of dihydrofolic acid in assay buffer was prepared. The reactions were started by the addition of 60 µL of dihydrofolic acid to each well. Absorbance was measured immediately at 340 nm in kinetic mode at room temperature and obtained two values for the absorbance (A1 and A_2) at two-time points (t1 and t_2) in the linear range of the plot. The slope was calculated for all test inhibitor samples and enzyme control by dividing the net ΔA (A1 A2) values with the time Δt (t_1 t2). Subtract the background or inhibitor control readings from its paired sample readings.

$$\%\,\text{Inhibition} = \frac{\text{Slope of enzyme control} - \text{Slope of inhibitor sample}}{\text{Slope of enzyme control}} \text{ X } 100$$

The IC_{50} values were calculated by plotting a graph between percentage inhibition and the corresponding concentration of the compound. All results were performed in triplicates. The IC_{50} values were indicated as mean ± SD.

2.6. In silico study

2.6.1. Molecular docking

Study of molecular docking was elucidated using Molecular Operating Environment (MOE) version 2019.01 software (https://www.chemcomp.com) and it is a rigid molecular docking software [69]. Studies of molecular docking have a high significance for predicting the probable binding modes of the tested active morpholine-thiazole hybrids against DHFR enzyme from *E. coli* (PDB ID: 1RF7). MOE is an interactive molecular graphics software which could calculate and show feasible docking modes of the target enzyme and the tested bis(pyrazoles). It requires the tested compounds and the target enzyme as input in PDB format. The molecules of water, co-crystallized ligands and other unsupported

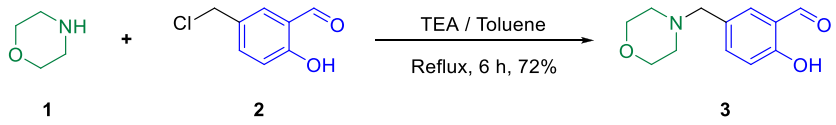

Scheme 1. Synthesis of benzaldehyde derivative 3 with a morpholine unit.

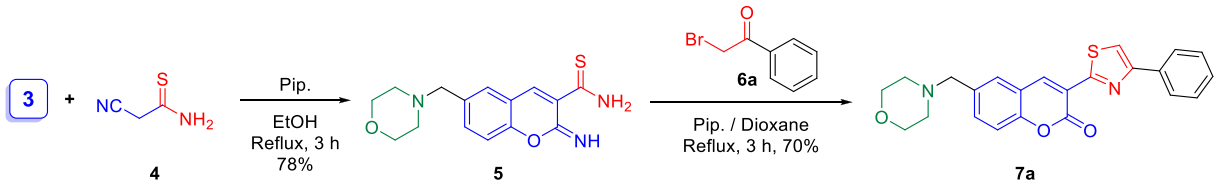

Scheme 2. Synthesis of thiazole-chromene hybrid 7a.

elements (e.g., Na, Mg, SO_4 etc.,) were removed but the amino-acid chain was reserved [70]. The ligand's structure in PDB file format was created by Gaussian 03 software. The structure of DHFR enzyme from *E. coli* was downloaded from the protein data bank (https://www.rcsb.org/).

2.6.2. ADME prediction

Computational studies of new hybrids **9a 9e** were performed to predict molecular properties using the SwissADME online server. The hybrids were drawn using ChemDraw Professional 16.0.0.82 [72]. Next, all hybrids were inserted into the SwissADME program to predict all the physicochemical characteristics, lipophilicity, solubility, pharmacokinetics, drug likeness, and medicinal chemistry [73]. The program provides predictions of the molecular weight, logarithm of partition coefficient (log P), number of hydrogen-bond donors, number of hydrogen-bond acceptors, number of rotatable bonds, topological polar surface area, and Lipinski's rule of five of the new synthesized hybrids. In addition, SwissADME was used to estimate the BOILED-Egg diagram that works by computing the polarity (TPSA) and lipophilicity (WLOGP) of small molecules [74]. Graphical estimations of human gastrointestinal absorption (HIA) and blood-brain barrier (BBB) penetration of the new hybrids.

3. Results and discussion

3.1. Chemistry

In the current study, the precursor 2–hydroxy-5-(morpholinomethyl)benzaldehyde **3** was synthesized and used as a key synthon for the synthesis of the target thiazole and thiazole-chromene hybrids with a morpholine unit. Therefore, morpholine **1** was reacted with 5-(chloromethyl)−2-hydroxybenzaldehyde **2** in boiling toluene at reflux in the presence of triethylamine (TEA) to afford benzaldehyde derivative **3** in a good yield (Scheme 1) [75,76].

TLC analyses were used to monitor all reactions used in this study in order to prepare the desired products in a pure state. At first, we investigated the synthesis of the carbothioamide derivative **5**, linked to chromene-morpholine hybrid, utilizing benzaldehyde derivative **3**. Thus, compound **3** was reacted with 2-cyanothioacetamide **4** in ethanol containing drops of piperidine at reflux for 3 h to give the corresponding 2-imino-6-(morpholinomethyl)−2*H*-chromene-3-carbothioamide **5** (Scheme 2 and Experimental section) [77,78]. Next, carbothioamide **5** was reacted with 2–bromo-1-phenylethan-1-one **6a** in dioxane containing drops of piperidine. TLC analysis revealed that heating the reaction mixture at reflux for 3 h was sufficient to yield the target 6-(morpholinomethyl)−3-(4-phenylthiazol-2-yl)−2*H*-chromen-2-one **7a** as a sole product (Scheme 2) [77,79]. The structure was elucidated by considering its elemental as well as spectral analyses. Its ^{1}H NMR spectrum revealed two triplet signals at δ 2.40 and 3.60 owing to morpholine protons. In addition, it showed four singlet signals at δ 3.65, 7.66, 7.93 and 8.34 attributed to CH_2, chromene-H5, thiazole-H and chromene-H4 protons, respectively. Furthermore, it revealed a multiplet signal at δ 7.22–7.85 corresponding to five aromatic, chromene-H7 and chromene-H8 protons. Its ^{13}C NMR spectrum showed four signals at δ 53.5, 60.6, 66.3 and 164.6 owing to morpholine-C3, CH_2, morpholine-C2 and chromene-CO carbons, respectively. Additionally, it revealed 15 signals attributed to chromene, thiazole and aromatic carbons (Experimental part).

Table 1
Optimizing the yield of chromene-thiazole hybrid **7a**.

Entry	*Solvent	Catalyst	Time (h)	Yield (%)
1	Water	TEA	8	Traces
2	Water	Piperidine	8	Traces
3	Benzene	TEA	8	14
4	Benzene	DEA	8	10
5	Benzene	Piperidine	8	14
6	Toluene	TEA	8	22
7	Toluene	DEA	8	18
8	Toluene	Piperidine	8	20
9	Ethanol	TEA	7	59
10	Ethanol	Piperidine	7	55
11	DMF	TEA	6	65
12	DMF	DEA	6	60
13	DMF	Piperidine	6	62
14	Dioxane	TEA	6	85
15	Dioxane	DEA	6	70
16	Dioxane	Piperidine	6	74
17	Dioxane	TEA	8	85

* All reactions were carried out at reflux.

Recently, the multi-component reaction (MCR) has become an important tool for the synthesis of poly functionalized heterocyclic hybrids [80]. Some of the benefits of this technique are simplicity, shorter time of reaction, enhanced efficiency and reduced formation of the by-products with the production of diverse "drug-like" hybrids incorporating heterocyclic units [81,82]. Therefore, we investigated the synthesis of the target thiazole-chromene hybrid **7a** using a one-pot protocol. The reaction was carried out using the precursors benzaldehyde derivative **3**, 2-cyanothioacetamide **4** and 2bromo-1-phenylethan-1-one **6a** under different reaction conditions to prepare the target **7a** with a maximum yield and minimum reaction time (Scheme 3 and Table 1).

Each of piperidine, diethylamine (DEA) and TEA were investigated as basic catalysts for the one-pot synthesis of **7a** and in the presence of different polar or non-polar solvents. TLC analyses revealed that using of water as a polar solvent afforded only traces of **7a** (Table 1 and entries 1 and 2). Using of benzene or toluene as

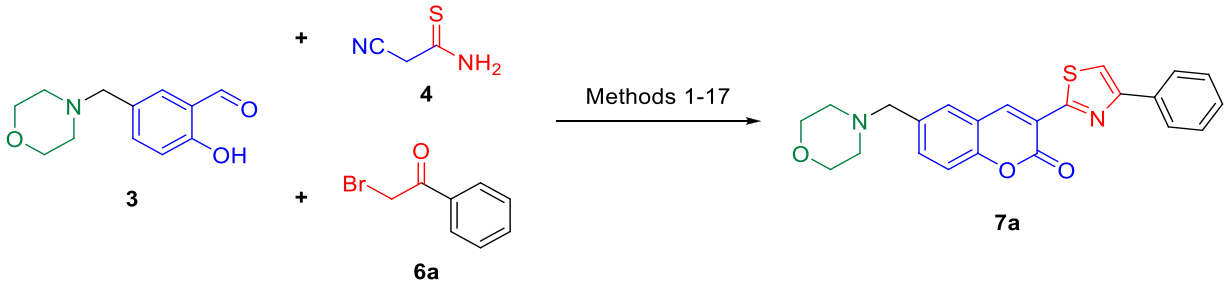

Scheme 3. One-pot synthesis of thiazole-chromene hybrid 7a.

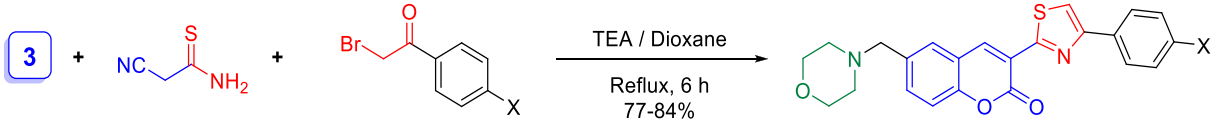

6b, X = Cl **c**, X = Br
d, X = Me; **e**, X = OMe

7b, X = Cl **c**, X = Br
d, X = Me; **e**, X = OMe

Scheme 4. One-pot synthesis of thiazole-chromene hybrids 7b 7e.

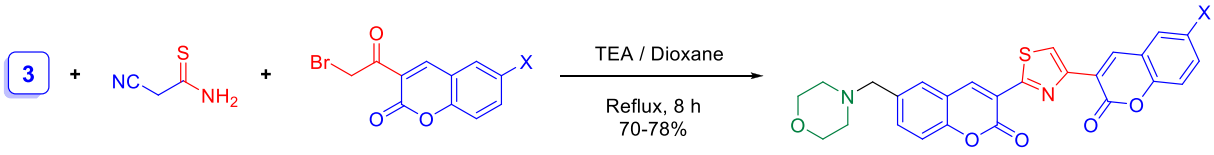

8a, X = H; **b**, X = Cl
c, X = Br; **d**, X = Me
e, X = OMe

9a, X = H; **b**, X = Cl
c, X = Br; **d**, X = Me
e, X = OMe

Scheme 5. One-pot synthesis of thiazole hybrids 9 utilizing α-bromoketones 8 linked to chromene units.

non-polar solvents afforded only 10–22% yields of **7a** (Table 1 and entries 3–8). The action of the former basic catalysts was also investigated in the presence of other polar solvents such as ethanol and dimethylformamide (DMF) to give **7a** in 55–65% yields (Table 1 and entries 9–13). Furthermore, using of dioxane as a solvent was investigated (Table 1 and entries 14–17). As seen in Table 1, it was clear that the best yield of **7a** was obtained by carrying out the reaction in dioxane in the presence of TEA as a catalyst at reflux for 6 h. This last method afforded a pure sample of **7a** with high purity in 85% yield (Table 1 and entry 14).

Using the optimized conditions used for the preparation of **7a**, a new series of chromene-thiazole hybrids **7b 7e** was prepared using the appropriate 1-aryl-2-bromoethan-1-one **6b-** instead of 2–bromo-1-phenylethan-1-one **6a** (Scheme 4 and Experimental section).

Furthermore, we examined the utility of α-bromoketones with a chromene unit, as versatile synthons for the preparation of the target chromene-thiazole hybrids. Therefore, the one-pot reaction of 2–hydroxy-5-(morpholinomethyl)benzaldehyde **3**, 2-cyanothioacetamide **4** and the appropriate 3-(2-bromoacetyl)−2*H*-chromen-2-ones **8a 8e** in dioxane in the presence of TEA as a catalyst. In all cases, heating the reaction mixture at reflux for 8 h resulted in the formation of the corresponding thiazole hybrids **9a 9e** as sole products as detected by TLC analyses (Scheme 5 and Experimental section).

3.2. Biology

3.2.1. Antibacterial activity: in vitro assay

3.2.1.1. MIC evaluation against standard susceptible ATCC strains. The in vitro antibacterial activities of the new morpholine-thiazole hybrids were estimated against six different Gram-positive and negative bacterial strains. For this purpose, the Gram-positive bacterial strains of *Staphylococcus aureus* (ATCC:6538), *Streptococcus mutans,* (ATCC:25,175) and *Enterococcus faecalis* (ATCC:29,212) as well as the Gram-negative bacterial strains of *E. coli* (ATCC:9637), *Pseudomonas aeruginosa* (ATCC:27,953) and *Klebsiella pneumonia* (ATCC:10,031) were selected. To estimate the MIC values for the new derivatives against the selected bacterial strains, the microbroth serial dilution method was used [62,63]. The minimum inhibitory concentration (MIC) values were recorded using the reference ciprofloxacin (MIC values of 2.7 μM against all the tested bacteria). All findings were listed in Table 2.

The precursor 2*H*-chromene-3-carbothioamide **5** showed MIC values of 25.7 μM against each of *S. aureus, S. mutans* and *E. coli* strains. Nonetheless, compound **5** revealed decreased antibacterial activities against the other tested strains with MIC values of 206.0 to more than 300 μM. The tested thiazole hybrids showed diverse antibacterial activities against the tested strains.

In our continuous study to prepare new morpholine-thiazole hybrids of potential antibacterial efficacies, we described herein the synthesis of two different series of thiazole hybrids. In each series, five hybrids were prepared attached to substituents of different electronic properties.

The first series of target hybrids **7a 7e** was prepared by attaching a chromene and an arene unit to thiazole-C2 and C4, respectively. The previous series showed, generally, low antibacterial activities against all the tested strains. Regarding the *S. aureus, S. mutans* and *E. coli* strains, hybrids **7** exhibited MIC values in the range of 35.9 to 77.1 μM. In addition, the prior hybrids displayed poor antibacterial activities against the *E. faecalis, P. aeruginosa* and *K. pneumonia* strains with MIC values in the range of 287.6 to more

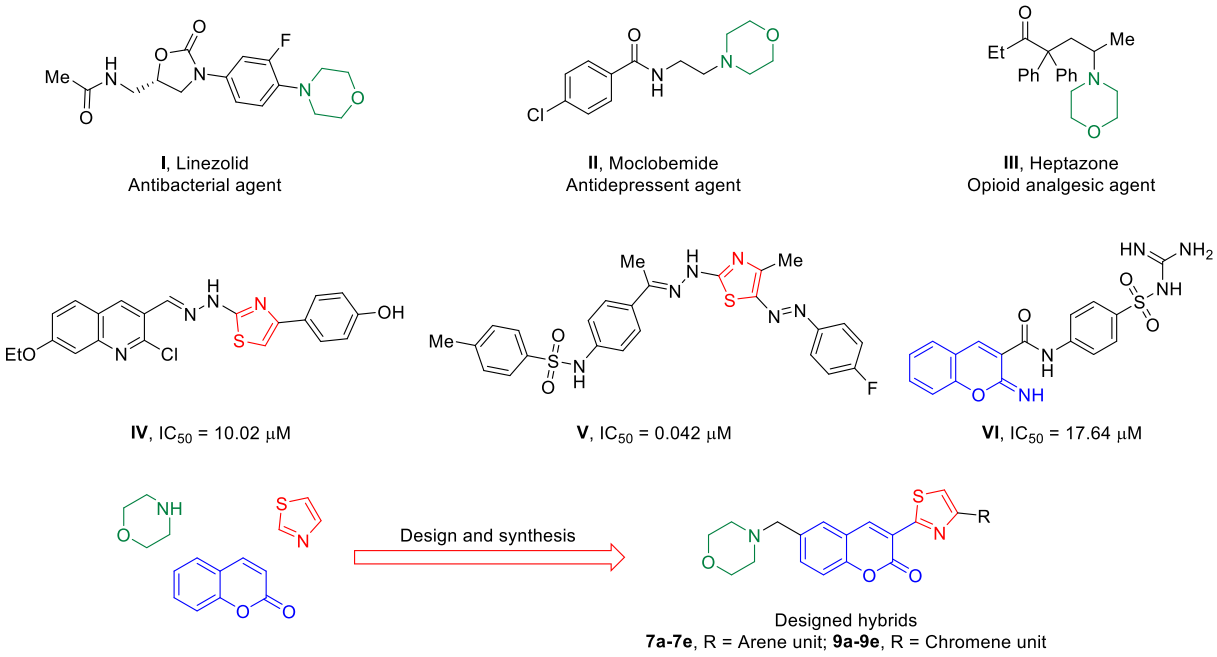

Fig. 1. Structure of some important morpholine-based drugs I-III and promising DHFR inhibitors IV-VI, as well as the designed hybrids 7 and 9.

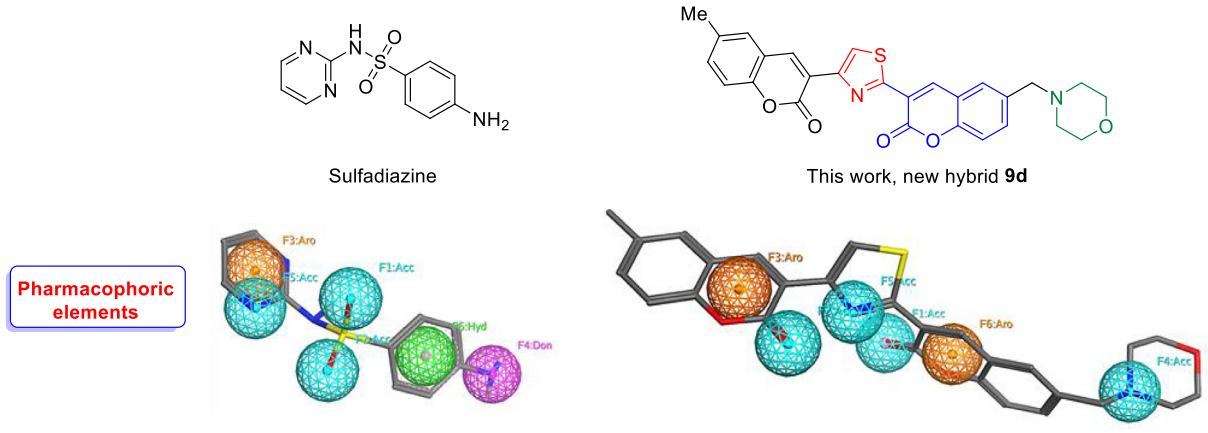

Fig. 2. Pharmacophoric elements of the reference sulfadiazine and the designed hybrid 9d [Blue (Acc)/violet (Don), hydrogen bond acceptor/donor; green (Hyd)/orange (Aro), hydrophobic/aromatic ring].

Table 2
MIC values in μM of new morpholine-thiazole hybrids.

Compound	MIC in μM					
	Gram-positive bacterial strains			Gram-negative bacterial strains		
Compound	*S. aureus*	*S. mutans*	*E. faecalis*	*E. coli*	*P. aeruginosa*	*K. pneumonia*
5	25.7	25.7	206.0	25.7	206.0	> 300
7a	38.5	77.1	> 300	38.5	> 300	> 300
7b	71.0	71.0	> 300	71.0	> 300	> 300
7c	64.5	64.5	> 300	64.5	> 300	> 300
7d	37.2	37.2	298.6	37.2	298.6	> 300
7e	35.9	35.9	287.6	35.9	287.6	287.6
9a	8.2	16.5	66.0	8.2	66.0	66.0
9b	15.3	30.7	123.2	30.7	123.1	246.4
9c	14.1	28.2	113.3	28.2	113.3	113.3
9d	3.9	3.9	16.0	3.9	16.0	32.0
9e	1.7	1.7	15.5	1.7	15.5	15.5
Ciprofloxacin	2.7	2.7	2.7	2.7	2.7	2.7

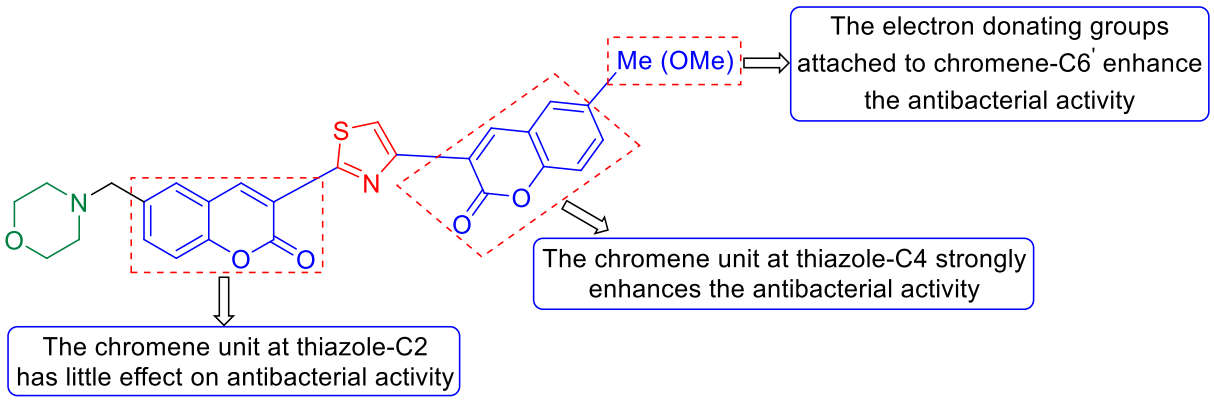

Fig. 3. Structure of some important morpholine-based drugs.

Table 3
MBC values in μM of some new morpholine-thiazole hybrids against each of *S. aureus, S. mutans* and *E. coli* strains.

	MBC in μM		
Compound	*S. aureus*	*S. mutans*	*E. coli*
9a	16.5	16.5	16.5
9b	30.7	61.4	30.7
9c	28.2	56.4	28.2
9d	7.8	7.8	7.8
9e	3.5	3.5	3.5
Ciprofloxacin	5.4	5.4	5.4

Table 4
MIC and MBC values in μM of some new morpholine-thiazole hybrids against ATCC:33,591 and ATCC:43,300 MRSA strains.

	MRSA (ATCC:33,591)		MRSA (ATCC:43,300)	
Compound	MIC	MBC	MIC	MBC
9a	66.0	132.0	33.0	66.0
9b	123.2	246.5	61.5	123.2
9c	113.3	226.6	113.3	113.3
9d	32.0	64.1	16.0	32.0
9e	15.5	31.0	7.7	15.5
Linezolid	5.2	46.2	2.6	46.2

than 300 μM. In conclusion, incorporation of a chromene unit at thiazole-C2 has low effect on the antibacterial activities of the target hybrids.

Motivated by the afore-mentioned findings, a second series of the morpholine-thiazole hybrids **9a 9e** with two chromene units at thiazole-C2 and thiazole-C4 was prepared. Among all tested compounds, in general, the prior series showed enhanced antibacterial efficacies. Compound **9e**, linked to methoxy group, exhibited the best antibacterial activity against *S. aureus, S. mutans* and *E. coli* strains (MIC value = 1.7 μM) which is exceeding that of the reference ciprofloxacin (MIC value = 2.7 μM). In addition, compound **9d**, linked to methyl group, was the second-best antibacterial agent with MIC value of 3.9 μM against these three strains. However, hybrids **9a 9c** show less potency with MIC values ranging between 8.2 and 30.7 μM against the same three strains. On the other hand, all **9a 9e** hybrids exhibited less antibacterial activities against *E. faecalis, P. aeruginosa* and *K. pneumonia* strains with the activities are slightly better for hybrids **9d** and **9e** (MIC values in the range of 15.5 to 32.0 μM), compared to hybrids **9a 9c** (MIC values in the range of 66.0 to 123.1 μM).

In conclusion, incorporating a chromene unit at thiazole-C4 significantly improves the antibacterial activities of the desired thiazole hybrids. Furthermore, the presence of strong electron donating groups such as methyl and methoxy groups attached to the preceding chromene unit at C6′ improves the antibacterial activity against all of the tested hybrids. All of the findings are summarized in Fig. 3.

3.2.1.2. MBC evaluation against standard susceptible ATCC strains. Thiazole hybrids **9a 9e** displayed the best antibacterial efficacies against each of *E. coli* (ATCC:9637), *S. mutans* (ATCC:25,175) and *S. aureus* (ATCC:6538) strains. These hybrids were subjected to the evaluation of their minimum bactericidal concentration (MBC) values against the prior strains [65]. All findings were recorded using ciprofloxacin as the reference drug (MBC values of 5.4 μM against all the tested strains) (Table 3).

Thiazole derivative **9e** displayed more powerful efficacy against all the tested bacterial strains than the reference ciprofloxacin. It exhibited MBC values of 3.5 μM against each of *E. coli, S. mutans* and *S. aureus* strains. Again, thiazole derivative **9d** was the second best in antibacterial efficacy with MBC values of 7.8 μM against the prior strains. Other thiazole derivatives **9a 9c** displayed low efficacies with MBC values in the range of 16.5 to 61.4 μM.

In general, all of the tested hybrids' MBC values are equal to or twice their MIC values against the same bacterial strains. This implies that all of the hybrids tested are bactericidal agents.

3.2.1.3. Assessment of antibacterial activity against MRSA strains. Inspired by the findings of antibacterial assessment against *Staphylococcus aureus* strain, some of new hybrids were examined as potential inhibitors of methicillin-resistant Staphylococcus aureus (MRSA) strains [37]. In this regard, the inhibitory activity of thiazole hybrids **9a 9e** were examined against two different MRSA strains (ATCC:33,591 and ATCC:43,300). The results were recorded using linezolid as a standard drug. Linezolid exhibited MIC/MBC values of 5.2/46.2 and 2.6/46.2 μM against ATCC:33,591 and ATCC:43,300 strains, respectively (Table 4).

The best inhibitory activity was found for the hybrid **9e**. It gave MIC/MBC values of 15.5/31.0 and 7.7/15.5 μM against ATCC:33,591 and ATCC:43,300 MRSA strains, respectively. Thiazole **9d** exhibited less inhibitory activity with MIC/MBC values of 32.0/64.1 and 16.0/32.0 μM against ATCC:33,591 and ATCC:43,300 strains, respectively. Other thiazole hybrids **9a 9c** displayed the least inhibitory activities with MIC and MBC values in the range of 61.5 to 226.6 μM. Generally, the MBC values of the hybrids **9a 9e** are equal to or twice their MIC values against the same strains. This implies that hybrids **9a 9e** are bactericidal agents.

3.2.1.4. Evaluation of anti-biofilm activity. Thiazole hybrids **9a 9e** were chosen for further assessment of their inhibitory activity against bacterial biofilm [66]. The results were recorded using the standard ciprofloxacin with IC_{50} values of 4.3 ± 0.11,

Table 5
Bacterial biofilm inhibition (IC_{50} in μM ± SD) of some new morpholine-thiazole hybrids.

Compound	IC_{50} in μM ± SD		
	S. aureus	*S. mutans*	*E. coli*
9a	4.7 ± 0.14	4.8 ± 0.15	4.7 ± 0.13
9b	5.2 ± 0.17	5.1 ± 0.16	5.0 ± 0.16
9c	5.6 ± 0.18	5.9 ± 0.17	5.6 ± 0.17
9d	4.5 ± 0.12	4.6 ± 0.13	4.5 ± 0.11
9e	4.0 ± 0.10	4.2 ± 0.12	3.9 ± 0.11
Ciprofloxacin	4.3 ± 0.11	4.5 ± 0.13	4.2 ± 0.12

Table 6
The IC_{50} values (in μM ± SD) of some new thiazole hybrids against MCF-10A, MCF-7, Caco2 and HEPG2 cell lines.

Compound	IC_{50} in μM			
	MCF-10A	MCF-7	Caco2	HEPG2
9a	9.4 ± 0.23	8.0 ± 0.18	8.3 ± 0.17	8.7 ± 0.21
9b	9.6 ± 0.26	8.2 ± 0.19	8.4 ± 0.15	8.8 ± 0.22
9c	9.6 ± 0.28	8.4 ± 0.13	8.5 ± 0.17	8.9 ± 0.24
9d	9.2 ± 0.18	7.9 ± 0.14	8.1 ± 0.11	8.5 ± 0.19
9e	9.0 ± 0.21	7.6 ± 0.12	7.9 ± 0.14	8.3 ± 0.18
Doxorubicin	9.2 ± 0.25	7.9 ± 0.16	8.0 ± 0.19	8.4 ± 0.21

4.5 ± 0.13 and 4.2 ± 0.12 μM against *S. aureus* (ATCC:6538), *S. mutans* (ATCC:25,175) and *E. coli* (ATCC:9637) strains, respectively (Table 5). Thiazole **9e** displayed more powerful biofilm inhibitory activity than ciprofloxacin. It exhibited IC_{50} values of 4.0 ± 0.10, 4.2 ± 0.12 and 3.9 ± 0.11 μM against *S. aureus, S. mutans* and *E. coli* strains, respectively. Furthermore, other hybrids displayed IC_{50} values in the range of 4.5 to 5.9 μM.

3.2.2. The in vitro cytotoxicity evaluation

The neutral red uptake (NRU) assay was performed to assess the in vitro cytotoxic activities of hybrids **9a 9e** [67]. To achieve this goal, the human breast epithelial MCF-10A, the human breast carcinoma MCF-7, colon cancer Caco2, and liver hepatocellular carcinoma HEPG2 cell lines were chosen to assess the cytotoxicity of the new hybrids. All the results were compared with the reference doxorubicin having IC_{50} values of 7.9 ± 0.16, 8.0 ± 0.19, 8.4 ± 0.21 and 9.2 ± 0.25 μM against the cell lines of MCF-7, Caco2, HEPG2 and MCF-10A, respectively (Table 6).

Thiazole hybrid **9e** displayed more potent cytotoxic activities than doxorubicin. It exhibited IC_{50} values of 7.6 ± 0.12, 7.9 ± 0.14, 8.3 ± 0.18 and 9.0 ± 0.21 μM against the cell lines of MCF-7, Caco2, HEPG2 and MCF-10A, respectively. Other hybrids displayed IC_{50} values in the range of 7.9 to 9.6 μM against these cell lines

3.2.3. The in vitro enzyme inhibition of DHFR

DHFR is a ubiquitous enzyme which shows its presence in protists, plants and animals. In the folate metabolic pathway for thymidine biosynthesis (precursor for DNA replication), DHFR role is well known where, with the aid of NADPH, it is responsible for reducing dihydrofolate to tetrahydrofolate [83]. With its responsibility for generating DNA replication raw materials, DHFR inhibition forms the basis for the treatment of many infectious diseases and is the target of antibacterial drugs like trimethoprim [4].

The in vitro inhibitory activities of DHFR enzyme [68] were assessed for hybrids **9a 9e** using sulfadiazine as a reference (IC_{50} value is 0.138 ± 0.005 μM) (Table 7). Hybrids **9d** and **9e** displayed the same or more powerful DHFR inhibitory activity than the standard sulfadiazine with IC_{50} values of 0.131 ± 0.004 and 0.122 ± 0.004 μM, respectively. Furthermore, other hybrids **9a 9c** showed lower inhibitory potency with IC_{50} values in the range of 0.224 to 0.453 μM.

3.2.4. Molecular modeling of some new thiazoles

Out of 20 new thiazoles prepared in this study, we found that the thiazole-chromene hybrids **9d** and **9e** exhibited potent DHFR inhibitory activity. As a result, we decided to use molecular docking simulations as an in silico study tool to gain a better understanding of the structure-activity relationships of these hybrids *via* their binding with enzyme. The determined structures of the selected thiazole-chromene hybrids were docked with DHFR enzyme from *E. coli* (PDB ID: 1RF7). Computational docking studies were used to determine the binding energies of the previous interactions [84]. The docking findings thiazole-chromene hybrids **9b, 9d** and **9e** as well as the reference sulfadiazine are listed in Table 8.

The in silico study was conducted to predict the capability of the tested hybrids as potential inhibitors of DHFR enzyme. The ligand interactions of the reference sulfadiazine with DHFR are presented in Fig. 4. Docking of sulfadiazine revealed the presence of strong H-bonding interactions between the two sulfonyl-O atoms with GLY 15 and GLY 97 residues in DHFR enzyme (3.24 Å, −2.0 kcal/mol; 2.82 Å, −4.0 kcal/mol) and between pyrimidine-N atom with THR 46 (2.96 Å, −2.4 kcal/mol).

Experimental study found that morpholine-thiazole hybrids **9d** and **9e**, attached to two chromene units at thiazole-C2 and C4, had the most powerful inhibitory activity against *E. coli* DHFR enzyme. Figs. 5 and 6 represented the 2D and 3D ligand interactions of the prior hybrids with the target enzyme.

Some of thiazole hybrids **9** exhibited promising DHFR inhibitory activities. This is consistent with the previously published results by Alrohily et al. on thiazole-based derivatives [85]. Accounting for the superior DHFR inhibitory activity of the tested thiazoles **9d** and **9e** compared to sulfadiazine drug, docking study showed stronger ligand interactions between thiazoles **9d** and **9e** with the residues of amino acids in DHFR enzyme when compared with the reference sulfadiazine (Fig. 7).

Presence of morpholine unit in hybrids **9d** and **9e** enhances the interactions with amino acids residues of the target enzyme [86]. Hence, docking study revealed strong H-bonding interactions between morpholine-O atom with ARG 98 residue in DHFR enzyme in both **9d** (2.55 Å, −4.6 kcal/mol) and **9e** (2.40 Å, −5.2 kcal/mol).

We could observe the dependence of DHFR inhibitory activities of thiazoles **9** on the presence of chromene units attached to thiazole-C2 and C4 [87]. Regarding chromene unit attached to thiazole-C2, docking poses revealed strong H-bonding interactions between chromene-CO group with THR 46 residue in **9d** (2.71 Å, −2.9 kcal/mol) and **9e** (2.56 Å, −3.1 kcal/mol). In addition, docking pose of **9e** showed hydrophobic contacts (π-H) between the chromene unit with residue of HIS 45 (3.39 Å, −1.9 kcal/mol). Regarding a chromene unit attached to thiazole-C4, docking poses showed favorable H-bonding interactions between chromene-CO group with amino acid residue in DHFR enzyme as in **9d** with GLY 97 (3.01 Å, −2.6 kcal/mol); and in **9e** with GLY 15 (2.95 Å, −2.7 kcal/mol).

The ligand interactions of the reference hybrid **9b** with DHFR are presented in Fig. 8. Docking of **9b** revealed the presence of strong H-bonding interactions between the two chromene-CO groups with THR 46 and GLY 97 residues in DHFR enzyme (3.13 Å, −1.2 kcal/mol; 3.31 Å, −1.6 kcal/mol).

3.2.5. SwissADME predictions of some new hybrids

The data predicted for the physicochemical characteristics, lipophilicity, solubility, pharmacokinetics, drug likeness, and medicinal chemistry of new hybrids **9a 9e** evaluated by SwissADME (http://www.swissadme.ch) are given in Table S1 (see Electronic supplemental file) [73]. Hybrids **9a 9e** had molecular weights ranging from 472.51 to 551.41 g/mol, a number of rotatable bonds, and H-bond acceptors in the ranges of 4–5 and 7–8, respectively, with no H-bond donors. Furthermore, the previous hy-

Table 7
The IC_{50} (in µM ± SD) of DHFR inhibitory activity of the tested thiazoles.

Compound	9a	9b	9c	9d	9e	Sulfadiazine
IC_{50}	0.224 ± 0.006	0.336 ± 0.009	0.453 ± 0.012	0.131 ± 0.004	0.122 ± 0.004	0.138 ± 0.005

Table 8
Docking results of thiazole-chromene hybrids **9b, 9d** and **9e** as well as the reference sulfadiazine with *Escherichia coli* DHFR (PDB ID: 1RF7).

Compound	Ligand moiety	Site	Interaction	Distance (Å)	E (kcal/mol)
9b	O 33	N THR 46 (A)	H-acceptor	3.13	−1.2
	O 46	N GLY 97 (A)	H-acceptor	3.31	−1.6
9d	O 23	NH2 ARG 98 (A)	H-acceptor	2.55	−4.6
	O 33	N THR 46 (A)	H-acceptor	2.71	−2.9
	O 46	N GLY 97 (A)	H-acceptor	3.01	−2.6
9e	O 23	NH2 ARG 98 (A)	H-acceptor	2.40	−5.2
	O 33	N THR 46 (A)	H-acceptor	2.56	−3.1
	O 46	CA GLY 15 (A)	H-acceptor	2.95	−2.7
	6-ring	N HIS 45 (A)	Pi-H	3.39	−1.9
Sulfadiazine	O 15	CA GLY 15 (A)	H-acceptor	3.24	−2.0
	O 16	N GLY 97 (A)	H-acceptor	2.82	−4.0
	N 27	OG1 THR 46 (A)	H-acceptor	2.96	−2.4

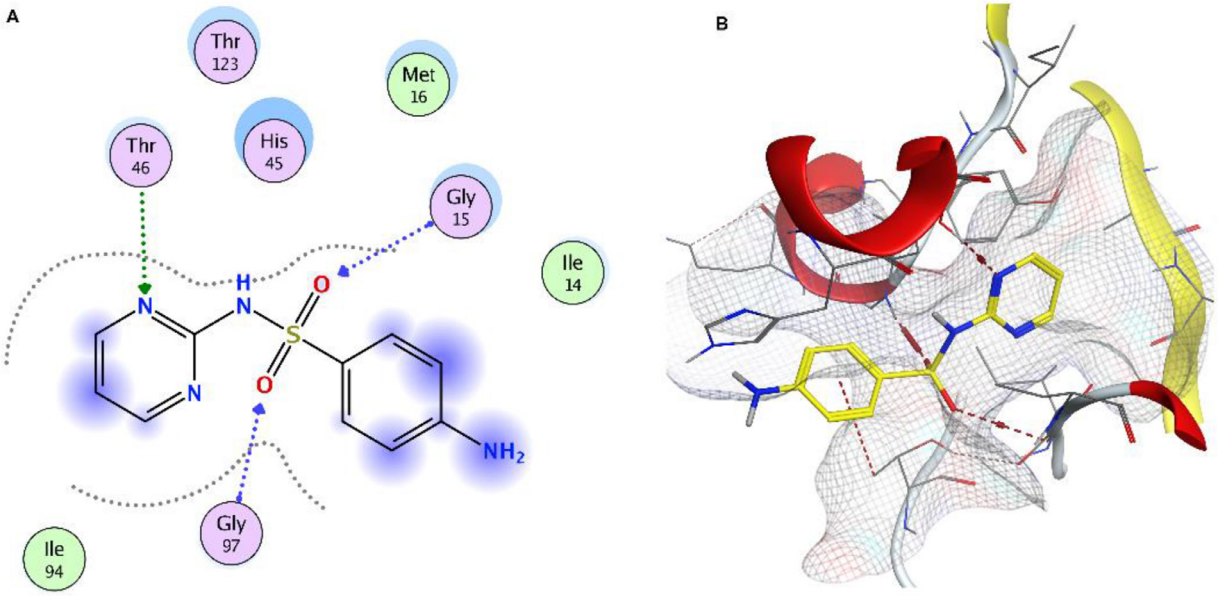

Fig. 4. 2D and 3D ligand interactions of sulfadiazine with *Escherichia coli* DHFR (1RF7).

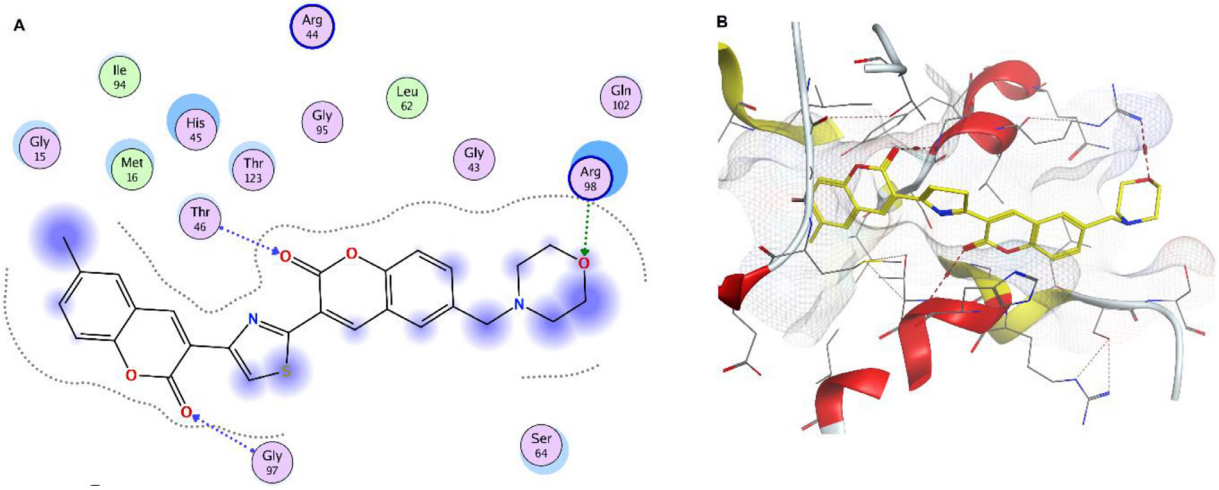

Fig. 5. A) 2D; and B) 3D ligand interactions of hybrid 9d with *Escherichia coli* DHFR (1RF7).

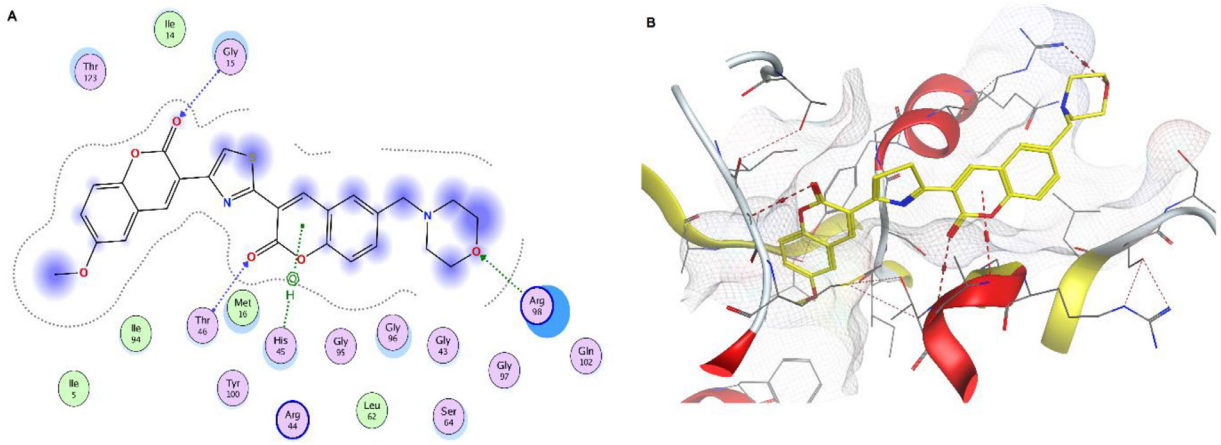

Fig. 6. A) 2D; and B) 3D ligand interactions of hybrid 9e with *Escherichia coli* DHFR (1RF7).

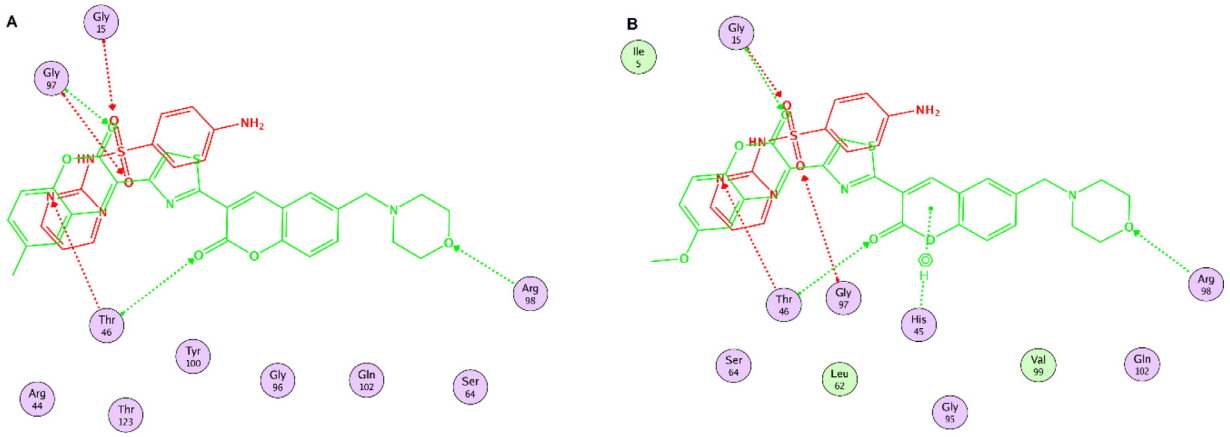

Fig. 7. The superposition of sulfadiazine (red, to the front) with either A) 9d (green, to the back); or B) 9e (green, to the back) inside the active site of DHFR (1RF7) structure.

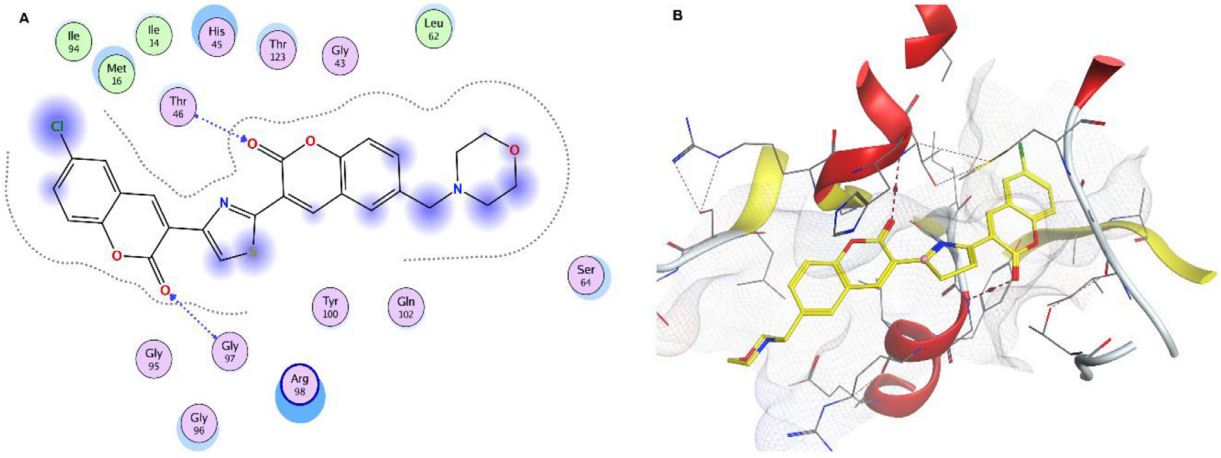

Fig. 8. A) 2D; and B) 3D ligand interactions of hybrid 9b with *Escherichia coli* DHFR (1RF7).

brids' topological polar surface area (TPSA) ranged from 114.02 to 123.25 Å^2.

The descriptor for lipophilicity is the partition coefficient between octanol and water (log $P_{o/w}$) that has a critical importance for pharmacokinetics drug discovery [88]. The SwissADME provides access to five predictive models, including XLOGP3 [89] and WLOGP [90]. The tested hybrids showed XLOGP3 and WLOGP in the ranges of 3.73–4.42 and 3.99–4.75, respectively. Furthermore, all tested hybrids, with the exception of **9c**, demonstrated water solubility log S < 6 (ESOL model) [91], which are favorable for bioavailable drugs.

Lipinski's rule of five rule states that there is no more than one violation of the following physicochemical parameters by orally active drugs: the molecular weight of the tested ligands ≤ 500, their H-bonding donors ≤ 5, H-bonding acceptors ≤ 10 and log $P_{o/w}$ ≤ 5 [92]. Only one violation of the above parameters (molecular weights > 500) was found in hybrids **9b, 9c**, and **9e**, while hybrids **9a** and **9d** showed no violations. As a result, all tested

hybrids were classified as drug-like. However, because of two violations of lead-likeness (molecular weights > 350 and XLOGP3 > 3.5) [93], all hybrids are not considered lead-like.

The BOILED-Egg method is a graphical model that works by computing the polarity (TPSA) and lipophilicity (WLOGP) of small molecules [74]. Graphical estimations of human gastrointestinal absorption (HIA) and blood-brain barrier (BBB) penetration of the new hybrids are shown in Figure S1. According to the BOILED-Egg diagram (see Electronic supplemental file), all tested hybrids showed high gastrointestinal absorption (GI) region with no permeability to the BBB. All hybrids could be P-glycoprotein substrates, reducing its absorption and penetration in the brain. All of these compounds have the potential to be promising agents that can be easily absorbed by the gastrointestinal tract while avoiding potential BBB permeability. These compounds do not cause central nervous system depression or drowsiness as side effects because they cannot cross the BBB [94].

In regards of the other pharmacokinetics of the tested hybrids, the SwissADME predicts the interaction of small molecules with cytochromes P450 (CYP1A2, CYP2C19, CYP2C9, CYP2D6, CYP3A4). Inhibition of the previous isoenzymes is a major cause of pharmacokinetics-related drug-drug interactions [95], resulting in toxic or other undesirable adverse effects due to the decreased clearance and accumulation of the drug or its metabolites [96]. All tested hybrids showed potential inhibition of CYP2C9 and CYP3A4.

4. Conclusion

A one-pot reaction protocol was adopted to prepare two different series of chromene-thiazole hybrids linked to a morpholine unit. The protocol involved reacting of the appropriate aldehyde, 2-cyanothioacetamide and α-bromoketones in dioxane in the presence of triethylamine. The series of thiazole hybrids, attached to two chromene units at thiazole-C2 and C4, demonstrated good antibacterial activity against the *S. aureus, S. mutans* and *E. coli* strains as well as MRSA strains tested. Thiazole hybrids **9d** and **9e** gave the best bacterial biofilm inhibitory efficacies against the *S. aureus, S. mutans* and *E. coli* strains with IC_{50} values ranging from 3.9 to 4.6 µM. The prior hybrids displayed more powerful DHFR inhibitory activity than the standard sulfadiazine with IC_{50} values of 0.131 and 0.122 µM, respectively. In silico SwissADME and molecular docking studies were used to determine the drug-likeness and the binding energies of some new hybrids with DHFR, respectively.

Declaration of Competing Interest

The authors declare no conflict of interest.

Supplementary materials

Supplementary material associated with this article can be found, in the online version, at doi:10.1016/j.molstruc.2021.131476.

CRediT authorship contribution statement

Sherif M.H. Sanad: Conceptualization, Methodology, Investigation, Writing – review & editing, Data curation, Supervision. **Ahmed E.M. Mekky:** Investigation, Validation, Writing – review & editing, Project administration, Software, Visualization. **Tamer T. El-Idreesy:** Investigation, Resources, Formal analysis, Writing – original draft.

References

[1] B.I. Schweitzer, A.P. Dicker, J.R. Bertino, Dihydrofolate reductase as a therapeutic target, FASEB J 4 (1990) 2441–2452, doi:10.1096/fasebj.4.8.2185970.
[2] M.V. Raimondi, O. Randazzo, M. La Franca, G. Barone, E. Vignoni, D. Rossi, S. Collina, D.H.F.R. Inhibitors, Reading the past for discovering novel anticancer agents, Molecules 24 (2019) 1140, doi:10.3390/molecules24061140.
[3] B. Srinivasan, S. Tonddast-Navaei, A. Roy, H. Zhou, J. Skolnick, Chemical space of *Escherichia coli* dihydrofolate reductase inhibitors: new approaches for discovering novel drugs for old bugs, Med. Res. Rev. 39 (2019) 684–705, doi:10.1002/med.21538.
[4] P. Singla, V. Luxami, K. Paul, Triazine–benzimidazole hybrids: anticancer activity, DNA interaction and dihydrofolate reductase inhibitors, Bioorg. Med. Chem. 23 (2015) 1691–1700, doi:10.1016/j.bmc.2015.03.012.
[5] P. Singh, M. Kaur, S. Sachdeva, Mechanism inspired development of rationally designed dihydrofolate reductase inhibitors as anticancer agents, J. Med. Chem. 55 (2012) 6381–6390, doi:10.1021/jm300644g.
[6] S. Hawser, S. Lociuro, K. Islam, Dihydrofolate reductase inhibitors as antibacterial agents, Biochem. Pharmacol. 71 (2006) 941–948, doi:10.1016/j.bcp.2005.10.052.
[7] D.A. Fidock, P.J. Rosenthal, S.L. Croft, R. Brun, S. Nwaka, Antimalarial drug discovery: efficacy models for compound screening, Nat. Rev. Drug Discov. 3 (2004) 509–520, doi:10.1038/nrd1416.
[8] N. Alsaad, R. van Altena, A.D. Pranger, D. van Soolingen, W.C.M. de Lange, T.S. van der Werf, J.G.W. Kosterink, J.-W.C. Alffenaar, Evaluation of co-trimoxazole in the treatment of multidrug-resistant tuberculosis, Eur. Respir. J. 42 (2013) 504–512, doi:10.1183/09031936.00114812.
[9] M.J. Boeree, D. Sauvageot, H.T. Banda, A.D. Harries, E.E. Zijlstra, Efficacy and safety of two dosages of cotrimoxazole as preventive treatment for HIV-infected Malawian adults with new smear-positive tuberculosis, Trop. Med. Int. Health. 10 (2005) 723–733, doi:10.1111/j.1365-3156.2005.01433.x.
[10] F.M. Huennekens, The methotrexate story: a paradigm for development of cancer chemotherapeutic agents, Adv. Enzyme Regul. 34 (1994) 397–419, doi:10.1016/0065-2571(94)90025-6.
[11] W. Song, P. Liu, M. Lei, H. You, X. Chen, H. Chen, L. Ma, L. Hu, $FeCl_3$ and morpholine as efficient cocatalysts for the one-step synthesis of quinoxalines from α-hydroxyketones and 1,2-diamines, Synth. Commun. 42 (2012) 236–245, doi:10.1080/00397911.2010.523489.
[12] S.P. Sawargave, A.S. Kudale, J.V. Deore, D.S. Bhosale, J.M. Divse, S.P. Chavan, H.B. Borate, One-step synthesis of 4-alkyl-3-aryl-2,6-dicyanoanilines and their use in the synthesis of highly functionalized 2,3,5,6,7- and 2,3,4,5,7-substituted indoles, Tetrahedron Lett. 52 (2011) 5491–5493, doi:10.1016/j.tetlet.2011.08.064.
[13] R. Wijtmans, M.K.S. Vink, H.E. Schoemaker, F.L. van Delft, R.H. Blaauw, F.P.J.T. Rutjes, Biological relevance and synthesis of c-substituted morpholine derivatives, Synthesis 2004 (2004) 641–662, doi:10.1055/s-2004-816003.
[14] C. Lin, P. Huang, C. Lu, R. Wu, W. Hu, J. Wang, Polygonapholine, an alkaloid with a novel skeleton, isolated from *Polygonatum alte-lobatum*, Tetrahedron 53 (1997) 2025–2028, doi:10.1016/S0040-4020(96)01165-9.
[15] Y. Minami, K. Yoshida, R. Azuma, M. Saeki, T. Otani, Structure of an aromatization product of C-1027 chromophore, Tetrahedron Lett. 34 (1993) 2633–2636, doi:10.1016/S0040-4039(00)77643-X.
[16] V.A. Pal'chikov, Morpholines. synthesis and biological activity, Russ. J. Org. Chem. 49 (2013) 787–814, doi:10.1134/S1070428013060018.
[17] U. Trstenjak, J. Ilaš, D. Kikelj, Advances in the synthesis of morpholin-3-ones and morpholin-2-ones, Synthesis 44 (2012) 3551–3578, doi:10.1055/s-0032-1316797.
[18] Q. Yang, L.G. Ulysse, M.D. McLaws, D.K. Keefe, B.P. Haney, C. Zha, P.R. Guzzo, S. Liu, Initial process development and scale-up of the synthesis of a triple reuptake inhibitor ALB 109780, Org. Process Res. Dev. 16 (2012) 499–506, doi:10.1021/op3000064.
[19] W. Xu, D.L. Gray, S.A. Glase, N.S. Barta, Design and synthesis of reboxetine analogs morpholine derivatives as selective norepinephrine reuptake inhibitors, Bioorg. Med. Chem. Lett. 18 (2008) 5550–5553, doi:10.1016/j.bmcl.2008.09.007.
[20] R.B. Rothman, M. Katsnelson, N. Vu, J.S. Partilla, C.M. Dersch, B.E. Blough, M.H. Baumann, Interaction of the anorectic medication, phendimetrazine, and its metabolites with monoamine transporters in rat brain, Eur. J. Pharmacol. 447 (2002) 51–57, doi:10.1016/S0014-2999(02)01830-7.
[21] D. Kim, D.H. Ryu, J.Y. Lee, N. Lee, Y. Kim, J. Kim, K. Chang, G. Im, T. Kim, W. Choi, Synthesis and biological evaluation of novel a-ring modified hexacyclic camptothecin analogues, J. Med. Chem. 44 (2001) 1594–1602, doi:10.1021/jm0004751.
[22] C. Guilloneau, Y. Charton, Y. Ginot, M. Fouquier-d'Hérouël, M. Bertrand, B. Lockhart, P. Lestage, S. Goldstein, Synthesis and pharmacological evaluation of new 1,2-dithiolane based antioxidants, Eur. J. Med. Chem. 38 (2003) 1–11, doi:10.1016/S0223-5234(02)01424-1.
[23] M.C. Chrysselis, E.A. Rekka, I.C. Siskou, P.N. Kourounakis, Nitric oxide releasing morpholine derivatives as hypolipidemic and antioxidant agents, J. Med. Chem. 45 (2002) 5406–5409, doi:10.1021/jm011062i.
[24] M.B. Tehrani, Z. Rezaei, M. Asadi, H. Behnammanesh, H. Nadri, F. Afsharirad, A. Moradi, B. Larijani, M. Mohammadi-Khanaposhtani, M. Mahdavi, Design, synthesis, and cholinesterase inhibition assay of coumarin-3-carboxamide-*n*-morpholine hybrids as new anti-alzheimer agents, Chem. Biodivers. 16 (2019) e1900144, doi:10.1002/cbdv.201900144.
[25] N.Ö. Can, U.A. Çevik, B.N. Sağlık, Y. Özkay, Ö. Atlı, M. Baysal, Ü.D. Özkay, Ö.D. Can, Pharmacological and toxicological screening of novel benzimidazole-morpholine derivatives as dual-acting inhibitors, Molecules 22 (2017) 1374, doi:10.3390/molecules22081374.

[26] P.A. Burland, H.M.I. Osborn, A. Turkson, Synthesis and glycosidase inhibitory profiles of functionalised morpholines and oxazepanes, Bioorg. Med. Chem. 19 (2011) 5679–5692, doi:10.1016/j.bmc.2011.07.019.

[27] S. Bera, G. Panda, I_2-mediated diversity oriented diastereoselective synthesis of amino acid derived *trans*-2,5-disubstituted morpholines, piperazines, and thiomorpholines, ACS Comb. Sci. 14 (2012) 1–4, doi:10.1021/co200129t.

[28] A. Trabocchi, A. Krachmalnicoff, G. Menchi, A. Guarna, Synthesis and conformational studies of a hybrid β-alanine–morpholine tetramer, Tetrahedron 68 (2012) 9701–9705, doi:10.1016/j.tet.2012.09.044.

[29] D.P. Walker, B.M. Eklov, M.W. Bedore, Practical synthesis of 3-oxa-6-azabicyclo[3.1.1]heptane hydrotosylate; a novel morpholine-based building block, Synthesis 44 (2012) 2859–2862, doi:10.1055/s-0032-1316748.

[30] M. Haroun, C. Tratrat, E. Tsolaki, A. Geronikaki, Thiazole-based thiazolidinones as potent antimicrobial agents. design, synthesis and biological evaluation, Comb. Chem. High Throughput Screen 19 (2016) 51–57, doi:10.2174/1386207319666151203002348.

[31] S.A. Rostom, I.M. El-Ashmawy, H.A. Abd El Razik, M.H. Badr, H.M. Ashour, Design and synthesis of some thiazolyl and thiadiazolyl derivatives of antipyrine as potential non-acidic anti-inflammatory, analgesic and antimicrobial agents, Bioorg. Med. Chem. 17 (2009) 882–895, doi:10.1016/j.bmc.2008.11.035.

[32] E.L. Luzina, A.V. Popov, Synthesis and anticancer activity of *N*-bis(trifluoromethyl)alkyl-*N*′-thiazolyl and *N*-bis(trifluoromethyl)alkyl-*N*′-benzothiazolyl ureas, Eur. J. Med. Chem. 44 (2009) 4944–4953, doi:10.1016/j.ejmech.2009.08.007.

[33] G. Turan-Zitouni, P. Chevallet, F.S. Kilic, K. Erol, Synthesis of some thiazolylpyrazoline derivatives and preliminary investigation of their hypotensive activity, Eur. J. Med. Chem. 35 (2000) 635–641, doi:10.1016/S0223-5234(00)00152-5.

[34] M. Khan, S. Hameed, T. Akhtar, N.A. Al-Masoudi, W.A. Al-Masoudi, P.G. Jones, C. Pannecouque, Synthesis, crystal structure, anti-HIV, and antiproliferative activity of new oxadiazole and thiazole analogs, Med. Chem. Res. 25 (2016) 2399–2409, doi:10.1007/s00044-016-1669-9.

[35] A. Zablotskaya, I. Segal, S. Germane, I. Shestakova, I. Domracheva, A. Nesterova, A. Geronikaki, E. Lukevics, Silyl modification of biologically active compounds. 8. trimethylsilyl ethers of hydroxyl-containing thiazole derivatives, Chem. Heterocycl. Compd. 38 (2002) 859–866, doi:10.1023/A:1020698107686.

[36] M. Britschgi, S. Greyerz, C. Burkhart, W.J. Pichler, Molecular aspects of drug recognition by specific T cells, Curr. Drug Targets 4 (2003) 1–11, doi:10.2174/1389450033347082.

[37] S.M.H. Sanad, A.E.M. Mekky, Synthesis, *in-vitro* antibacterial and anticancer screening of novel nicotinonitrile-coumarin hybrids utilizing piperazine citrate, Synth. Commun. 50 (2020) 1468–1485, doi:10.1080/00397911.2020.1743318.

[38] J.Y. Cho, T.L. Hwang, T.H. Chang, Y.P. Lim, P.J. Sung, T.H. Lee, J.J. Chen, New coumarins and anti-inflammatory constituents from *Zanthoxylum avicennae*, Food Chem 135 (2012) 17–23, doi:10.1016/j.foodchem.2012.04.025.

[39] I. Kostova, S. Bhatia, P. Grigorov, S. Balkansky, V.S. Parmar, A.K. Prasad, L. Saso, Coumarins as antioxidants, Curr. Med. Chem 18 (2011) 3929–3951, doi:10.2174/092986711803414395.

[40] H.M. Savanur, G.M. Pawashe, K.M. Kim, R.G. Kalkhambkar, Synthesis and molecular modeling studies of coumarin- and 1-aza-coumarin-linked miconazole analogues and their antifungal activity, ChemistrySelect 3 (2018) 9648–9653, doi:10.1002/slct.201801408.

[41] J. Neyts, E.D. Clercq, R. Singha, Y.H. Chang, A.R. Das, S.K. Chakraborty, S.C. Hong, S.C. Tsay, M.H. Hsu, J.R. Hwu, Structure−activity relationship of new anti-hepatitis c virus agents: heterobicycle−coumarin conjugates, J. Med. Chem 52 (2009) 1486–1490, doi:10.1021/jm801240d.

[42] A. Makowska, L. Wolff, F. Sączewski, P.J. Bednarski, A. Kornicka, Synthesis and cytotoxic evaluation of benzoxazole/benzothiazole-2-imino-coumarin hybrids and their coumarin analogues as potential anticancer agents, Pharmazie 74 (2019) 648–657, doi:10.1691/ph.2019.9664.

[43] S.M.H. Sanad, A.E.M. Mekky, Novel nicotinonitrile-coumarin hybrids as potential acetylcholinesterase inhibitors: design, synthesis, in vitro and in silico studies, J. Iran. Chem. Soc. 18 (1) (2021) 213–224, doi:10.1007/s13738-020-02018-6.

[44] A.E.M. Mekky, S.M.H. Sanad, Synthesis and in vitro study of new coumarin derivatives linked to nicotinonitrile moieties as potential acetylcholinesterase inhibitors, J. Heterocyclic Chem. 57 (2020) 4278–4290, doi:10.1002/jhet.4134.

[45] S.P. Hanlon, A. Camattari, S. Abad, A. Glieder, M. Kittelmann, S. Lütz, B. Wirz, M. Winkler, Expression of recombinant human flavin monooxygenase and moclobemide-*n*-oxide synthesis on multi-mg scale, Chem. Commun. 48 (2012) 6001–6003, doi:10.1039/C2CC17878H.

[46] J.D. More, Synthesis of the commercial antidepressant moclobemide, J. Chem. Educ. 85 (2008) 1424, doi:10.1021/ed085p1424.

[47] V.B. Lohray, B.B. Lohray, B.K. Srivastava, Novel anti-infective compounds, Pure Appl. Chem. 77 (2005) 195–200, doi:10.1351/pac200577010195.

[48] Y.A. Ammar, S.M. Abd El-Hafez, S.A. Hessein, A.M. Ali, A.A. Askar, A. Ragab, One-pot strategy for thiazole tethered 7-ethoxyquinoline hybrids: synthesis and potential antimicrobial agents as dihydrofolate reductase (DHFR) inhibitors with molecular docking study, J. Mol. Struct. 1242 (2021) 130748, doi:10.1016/j.molstruc.2021.130748.

[49] S.M. Riyadh, S.A. El-Motairi, H.E. Ahmed, K.D. Khalil, E.S.E. Habib, Synthesis, biological evaluation, and molecular docking of novel thiazoles and [1,3,4]thiadiazoles incorporating sulfonamide group as DHFR Inhibitors, Chem. Biodivers. 15 (2018) e1800231, doi:10.1002/cbdv.201800231.

[50] A. Ragab, S.A. Fouad, O.A.A. Ali, E.M. Ahmed, A.M. Ali, A.A. Askar, Y.A. Ammar, Sulfaguanidine hybrid with some new pyridine-2-one derivatives: design, synthesis, and antimicrobial activity against multidrug-resistant bacteria as dual DNA gyrase and DHFR inhibitors, Antibiotics 10 (2021) 162, doi:10.3390/antibiotics10020162.

[51] A.E.M. Mekky, S.M.H. Sanad, Synthesis, characterization, and antimicrobial evaluation of novel thiohydrazonates and pyrazolo[3,4-*b*]pyridines, Polycycl. Aromat. Compd. 41 (2021) 936–949, doi:10.1080/10406638.2019.1631194.

[52] S.M.H. Sanad, A.E.M. Mekky, New pyrido[3′,2′:4,5]thieno[3,2-*d*]pyrimidin-4(3*h*)-one hybrids linked to arene units: synthesis of potential mrsa, vre and cox-2 inhibitors, Can. J. Chem. Accept (Jun 10, 2021), doi:10.1139/cjc-2021-0121.

[53] S.M.H. Sanad, M.S.M. Ahmed, A.E.M. Mekky, Z.A. Abdallah, Regioselective synthesis and theoretical calculations of bis(pyrido[2′,3′:3,4]pyrazolo[1,5-*a*]pyrimidines) linked to benzofuran units *via* piperazine spacer: a DFT, MM2, and MMFF94 study, J. Mol. Struct. 1243 (2021) 130802, doi:10.1016/j.molstruc.2021.130802.

[54] M.A.M. Teleb, A.E.M. Mekky, S.M.H. Sanad, 3-aminothieno[2,3-*b*]pyridine-2-carboxylate: effective precursor for microwave assisted three components synthesis of new pyrido[3′,2′:4,5]thieno[3,2-*d*]pyrimidin-4(3*h*)-one hybrids, J. Heterocyclic Chem. 58 (9) (2021) 1825–1835, doi:10.1002/jhet.4313.

[55] S.M.H. Sanad, A.E.M. Mekky, A.A.M. El-Reedy, Tandem synthesis and antibacterial screening of novel thieno[2,3-*b*]thiophene-linked bis(thiazole) hybrids, Synth. Commun. 51 (13) (2021) 1982–1993, doi:10.1080/00397911.2021.1918170.

[56] S.M.H. Sanad, A.E.M. Mekky, A.Y. Said, M.A.A. Elneairy, Pyridine-2(1*H*)-thiones: versatile precursors for one-pot synthesis of new nicotinonitrile-thiazole hybrids, J. Heterocyclic Chem. 58 (7) (2021) 1461–1471, doi:10.1002/jhet.4272.

[57] I.A. Abdelhamid, M.A.E. Hawass, S.M.H. Sanad, A.H.M. Elwahy, Synthesis of various pyrazole-fused heterocyclic systems using pyrazole-4-carbaldehydes as versatile precursors, Arkivoc 2021 (9) (2021) 42–74, doi:10.24820/ark.5550190.p011.542.

[58] S.M.H. Sanad, A.E.M. Mekky, A.Y. Said, M.A.A. Elneairy, New thieno[2,3-*b*]pyridine-fused [1,2,4]triazolo[4,3-*a*]pyrimidinone hybrids as potential MRSA and VRE inhibitors, Mendeleev Commun. 31 (3) (2021) 370–372, doi:10.1016/j.mencom.2021.04.029.

[59] A.E.M. Mekky, S.M.H. Sanad, T.T. El-Idreesy, New thiazole and thiazole-chromene hybrids possessing morpholine units: piperazine-mediated one-pot synthesis of potential acetylcholinesterase inhibitors, Synth. Commun. (2021) Aug 17, doi:10.1080/00397911.2021.1970774.

[60] Y.S. Kiani, S. Kalsoom, N. Riaz, In silico ligand-based pharmacophore model generation for the identification of novel Pneumocystis carinii DHFR inhibitors, Med. Chem. Res. 22 (2013) 949–963, doi:10.1007/s00044-012-0082-2.

[61] T. Langer, G. Wolber, Pharmacophore definition and 3D searches, Drug Discov. Today Technol. 1 (2004) 203–207, doi:10.1016/j.ddtec.2004.11.015.

[62] A.E.M. Mekky, S.M.H. Sanad, Novel bis(pyrazole-benzofuran) hybrids possessing piperazine linker: synthesis of potent bacterial biofilm and murB inhibitors, Bioorg. Chem. 102 (2020) 104094, doi:10.1016/j.bioorg.2020.104094.

[63] H. Mohammad, P.N. Reddy, D. Monteleone, A.S. Mayhoub, M. Cushman, M.N. Seleem, Synthesis and antibacterial evaluation of a novel series of synthetic phenylthiazole compounds against methicillin-resistant Staphylococcus aureus (MRSA), Eur. J. Med. Chem. 94 (2015) 306–316, doi:10.1016/j.ejmech.2015.03.015.

[64] CLSI. 2012. Methods for dilution antimicrobial susceptibility tests for bacteria that grow aerobically-7th edition. Approved standard M07-A9, Clinical and Laboratory Standards Institute Wayne, PA.

[65] A. Kamal, A. Rahim, S. Riyaz, Y. Poornachandra, M. Balakrishna, C.G. Kumar, S.M. Hussaini, B. Sridhar, P.K. Machiraju, Regioselective synthesis, antimicrobial evaluation and theoretical studies of 2-styryl quinolines, Org. Biomol. Chem. 13 (2015) 1347–1357, doi:10.1039/C4OB02277G.

[66] R.E. Furlani, A.A. Yeagley, C. Melander, A flexible approach to 1,4-di-substituted 2-aminoimidazoles that inhibit and disperse biofilms and potentiate the effects of β-lactams against multi-drug resistant bacteria, Eur. J. Med. Chem. 62 (2013) 59–70, doi:10.1016/j.ejmech.2012.12.005.

[67] G. Repetto, A. Del Peso, J.L. Zurita, Neutral red uptake assay for the estimation of cell viability/cytotoxicity, Nat. Protoc. 3 (2008) 1125–1131, doi:10.1038/nprot.2008.75.

[68] N.H. Metwally, M.S. Mohamed, New imidazolone derivatives comprising a benzoate or sulfonamide moiety as anti-inflammatory and antibacterial inhibitors: design, synthesis, selective COX-2, DHFR and molecular-modeling study, Bioorg. Chem. 99 (2020) 103438, doi:10.1016/j.bioorg.2019.103438.

[69] Molecular Operating Environment (MOE), 2019.01; Chemical Computing Group ULC, 1010 Sherbooke St. West, Suite #910, Montreal, QC, Canada, H3A 2R7, 2021.

[70] M.M. Mysinger, B.K. Shoichet, Rapid context-dependent ligand desolvation in molecular docking, J. Chem. Inf. Model. 50 (2010) 1561–1573, doi:10.1021/ci100214a.

[71] http://www.swissadme.ch, Swiss institute of bioinformatics, Last Accessed on (2020) 10 Oct.

[72] ChemDraw Professional 16.0.0.82. https://www.perkinelmer.com/uk/product/chemdraw-professional-chemdrawpro.

[73] A. Daina, O. Michielin, V.A. Zoete, SwissADME: a free web tool to evaluate pharmacokinetics, drug-likeness and medicinal chemistry friendliness of small molecules, Sci. Rep. 7 (2017) 42717, doi:10.1038/srep42717.

[74] A. Daina, V.A. Zoete, A boiled-egg to predict gastrointestinal absorption and brain penetration of small molecules, ChemMedChem 11 (2016) 1117–1121, doi:10.1002/cmdc.201600182.

[75] S. Guieu, J. Rocha, A.M. Silva, Synthesis of unsymmetrical methylenebisphenol derivatives, Synlett 24 (2013) 762–764, doi:10.1055/s-0032-1318394.
[76] M. Shaker, A.S. Beni, Cu@SB-MCM-41 composite as an efficient and recyclable nanocatalyst for the synthesis of polyhydroquinoline derivatives via unsymmetrical Hantzsch reaction, J. Porous Mater. 28 (2021) 435–449, doi:10.1007/s10934-020-01006-8.
[77] S.M.H. Sanad, A.E.M. Mekky, Efficient synthesis and characterization of novel bis(chromenes) and bis(benzo[*f*]chromenes) linked to thiazole units, Synth. Commun. 51 (4) (2021) 611–624, doi:10.1080/00397911.2020.1846748.
[78] A.E.M. Mekky, S.M.H. Sanad, Synthesis of novel bis(chromenes) and bis(chromeno[3,4-*c*]pyridine) incorporating piperazine moiety, Synth. Commun. 49 (2019) 1385–1395, doi:10.1080/00397911.2019.1595658.
[79] A.E.M. Mekky, S.M.H. Sanad, Synthesis and antibacterial evaluation of novel mono- and bis(2*H*-chromen-2-imine) hybrids linked to heteroarene units, Mendeleev Commun. 30 (2020) 762–764, doi:10.1016/j.mencom.2020.11.024.
[80] I.A. Ibarra, A. Islas-Jácome, E. González-Zamora, Synthesis of polyheterocycles *via* multicomponent reactions, Org. Biomol. Chem. 16 (2018) 1402–1418, doi:10.1039/C7OB02305G.
[81] R.C. Cioc, E. Ruijter, R.V.A. Orru, Multicomponent reactions: advanced tools for sustainable organic synthesis, Green Chem. 16 (2014) 2958–2975, doi:10.1039/C4GC00013G.
[82] A. Kulkarni, B. Torok, Microwave-assisted multicomponent domino cyclization–aromatization: an efficient approach for the synthesis of substituted quinolines, Green Chem. 12 (2010) 875–878, doi:10.1039/C001076F.
[83] P. Singh, M. Kaur, S. Sachdeva, Mechanism inspired development of rationally designed dihydrofolate reductase inhibitors as anticancer agents, J. Med. Chem. 55 (2012) 6381–6390, doi:10.1021/jm300644g.
[84] G.M. Morris, R. Huey, W. Lindstrom, M.F. Sanner, R.K. Belew, D.S. Goodsell, A.J. Olson, AutoDock4 and autodocktools4: automated docking with selective receptor flexibility, J. Comput. Chem. 30 (2009) 2785–2791, doi:10.1002/jcc.21256.
[85] W.D. Alrohily, M.E. Habib, S.M. El-Messery, A. Alqurshi, H. El-Subbagh, E.S.E. Habib, Antibacterial, antibiofilm and molecular modeling study of some antitumor thiazole based chalcones as a new class of DHFR inhibitors, Microb. Pathog. 136 (2019) 103674, doi:10.1016/j.micpath.2019.103674.
[86] P. Wipf, W. Weiner, Enantioselective synthesis and photoracemization studies of (+)-2-cyclopropyl-7,8-dimethoxy-2*h*- chromene-5-carboxylic acid methyl ester, an advanced intermediate of a dihydrofolate reductase inhibitor, J. Org. Chem. 64 (1999) 5321–5324, doi:10.1021/jo990352s.
[87] Z.A. Muhammad, M.M. Edrees, R.A. Faty, S.M. Gomha, S.S. Alterary, Y.N. Mabkhot, Antitumor evaluation and molecular docking of new morpholine based heterocycles, Molecules 22 (2017) 1211, doi:10.3390/molecules22071211.
[88] J.A. Arnott, S.L. Planey, The influence of lipophilicity in drug discovery and design, Expert Opin. Drug Discov. 7 (2012) 863–875, doi:10.1517/17460441.2012.714363.
[89] T. Cheng, Y. Zhao, X. Li, F. Lin, Y. Xu, X. Zhang, Y. Li, R. Wang, L. Lai, Computation of octanol−water partition coefficients by guiding an additive model with knowledge, J. Chem. Inf. Model. 47 (2007) 2140–2148, doi:10.1021/ci700257y.
[90] S.A. Wildman, G.M. Crippen, Prediction of physicochemical parameters by atomic contributions, J. Chem. Inf. Model. 39 (1999) 868–873, doi:10.1021/ci990307l.
[91] J.S. Delaney, ESOL: estimating aqueous solubility directly from molecular structure, J. Chem. Inf. Model. 44 (2004) 1000–1005, doi:10.1021/ci034243x.
[92] C.A. Lipinski, Lead- and drug-like compounds: the rule-of-five revolution, Drug Discov. Today Technol. 1 (2004) 337–341, doi:10.1016/j.ddtec.2004.11.007.
[93] S. Teague, A. Davis, P. Leeson, T. Oprea, The design of leadlike combinatorial libraries, Angew. Chem. Int. Ed. 38 (1999) 3743–3748, doi:10.1002/(SICI)1521-3773(19991216)38:24⟨3743::AID-ANIE3743⟩3.0.CO;2-U.
[94] Y. Sicak, Design and antiproliferative and antioxidant activities of furan-based thiosemicarbazides and 1,2,4-triazoles: their structure-activity relationship and SwissADME predictions, Med. Chem. Res. 30 (2021) 1557–1568, doi:10.1007/s00044-021-02756-z.
[95] S.M. Huang, J.M. Strong, L. Zhang, K.S. Reynolds, S. Nallani, R. Temple, S. Abraham, S.A. Habet, R.K. Baweja, G.J. Burckart, S. Chung, New era in drug interaction evaluation: US food and drug administration update on cyp enzymes, transporters, and the guidance process, J. Clin. Pharmacol. 48 (2008) 662–670, doi:10.1177/0091270007312153.
[96] J. Kirchmair, A.H. Göller, D. Lang, J. Kunze, B. Testa, I.D. Wilson, R.C. Glen, G. Schneider, Predicting drug metabolism: experiment and/or computation? Nat. Rev. Drug Discov. 14 (2015) 387–404, doi:10.1038/nrd4581.